LUND UNIVERSITY

RS•C

Micro Total Analysis Systems 2004

Proceedings of μTAS 2004
8th International Conference on Miniaturized Systems
in Chemistry and Life Sciences
September 26-30, Malmö, Sweden

EDITORS: Thomas Laurell, Johan Nilsson,
Klavs Jensen, D. Jed Harrison and Jörg P. Kutter

Micro Total Analysis Systems 2004
Volume 1

Proceedings of μTAS 2004
8th International Conference on Miniaturized Systems for Chemistry and Life Sciences

Malmö, Sweden
September 26-30, 2004

edited by

Thomas Laurell
Lund Institute of Technology, Sweden

Johan Nilsson
Lund Institute of Technology, Sweden

Klavs Jensen
Massachusetts Institute of Technology, USA

D. Jed Harrison
University of Alberta, Canada

Jörg P. Kutter
Technical University of Denmark, Denmark

RS•C
advancing the chemical sciences

Special Publication No. 296

ISBN 0-85404-643-7

A catalogue record for this book is available from the British Library

Published by The Royal Society of Chemistry,
Thomas Graham House, Science Park, Milton Road,
Cambridge CB4 0WF, UK

Registered Charity Number 207890

For further information see our web site at www.rsc.org

Printed by Athenaeum Press Ltd, Gateshead, Tyne and Wear, UK

PREFACE

The 8th International Conference on Miniaturisation in Chemistry and Life Sciences, MicroTAS (Micro Total Analysis Systems) is celebrating its 10th anniversary year. The conference developed from a small gathering of researchers active in the field of MicroTAS in Enschede, The Netherlands, in 1994 with 160 participants. The success of this first meeting was followed by an equally appreciated μTAS workshop in Basel, Switzerland, in 1996 with a remarkable increase in the number of participants to 275. Optimism in the research field continued and the subsequent event was the truly unforgettable conference organised in Banff, Canada in 1998, with a record-breaking 420 conference delegates and about 130 papers submitted. At the following meeting in 2000, the conference returned to its birth place in Europe (at the University of Twente, Enschede, The Netherlands) again breaking new records for the MicroTAS conference with close to 500 attendees and about 140 scientific papers accepted (230 submissions). Due to the increasing interest that the MicroTAS/Lab-On-A-Chip field was generating, the subsequent meeting in 2001, in Monterey, CA, USA, forced the conference format into two parallel oral sessions in order to meet the pressure from the scientific community. In spite of the 9-11 terrorist attack and subsequent restrictions in international travelling, the conference attracted about 790 delegates and 276 accepted scientific contributions. The meeting was also characterised by an impressive commercial exhibition, demonstrating the transition of several of the earlier μTAS developments into the industrial sector. The subsequent conference (2002) in Japan is forever etched into our minds both with respect to the excellent organisation and scientific programme as well as the wonderful setting in ancient Nara. Although difficulties were developing in the industrial and financial sectors, following the IT-crash, the Nara meeting attracted 710 delegates with 316 accepted scientific contributions. The next μTAS conference was organised in another glorious location, Squaw Valley, CA, USA, in October 2003 and despite the setback in the global economy which clearly also affected academic budgets the conference attracted over 650 delegates with 325 accepted scientific presentations.

This year's conference confirms the continuing increase in interest in the μTAS-research field. More papers were submitted than ever before, 657, giving the Technical Programme Committee a difficult task in the abstract evaluation procedure. Again the scientific programme expanded, now to encompass a total of 422 accepted scientific contributions. We also see a continuing strong presence from the industrial area with some new players, indicating a recovery in the financial sector.

These two volumes contain the proceedings of the MicroTAS 2004 conference in Malmö, Sweden, September 26-30. Every paper presented will also be made available from the Royal Society of Chemistry, Lab on a Chip web-site at www.rsc.org/loc. The proceedings from the μTAS 2003 conference can also be accessed from this site.

The content of this year's MicroTAS conference clearly shows that the efforts in developing cell-based microsystems are increasing. Not only is work quite frequently focused on cell manipulation, and on-chip culturing but also on complete microsystems

for cell transport, culturing, analysis and monitoring including feed-back systems are now presented. The transition to polymer-based technologies continues and the now widely used SU-8/PDMS platform has opened up the μTAS-field to all those who do not necessarily have access to high performance clean-rooms, which vastly broadens the number of players that can now access and work in the field. A clear trend is also the increase in microfluidic two-phase systems, which seems to have come to a point where the two-phase fluid handling is well controlled and, *e.g.,* applications with compartmentalised chemistry in oil-immersed aqueous droplets in streaming microsystems are seen. The more mature areas of chip-based separation science are still very strong moving towards applications in genomics, proteomics and diagnostics. An exciting development is the continued progress in nanotechnology and the study of microfluidic transport, and molecular interaction and separation in nanoscale channels, this year displaying a representation equal to those in cell-based microsystems.

Looking back at μTAS conferences over the last ten years I can conclude that the field has matured and broadened from the original very strong focus on chip-based capillary electrophoresis systems to encompass a new science field of an extremely interdisciplinary nature with materials physicists and analytical chemists at one end and cell & molecular biologists and clinicians at the other. The field of microfluidics with all its aspects in combination with micro- and nanotechnology and life science research is accelerating, finding new areas where the miniaturised scale really makes a difference, and this is, of course, what research in this area is all about! We can confidently look forward to another ten years of exciting developments in this scientific field.

Finally, I would like to express my thanks to all of those who helped in organising this conference. The local organising committee for their broad network to industrial supporters and exhibitors and for all the work that is not seen but is yet so necessary. The Technical Programme Committee for the seemingly endless work reading and evaluating the 650 submitted abstracts in a medieval castle in southern Sweden. This is a task on which the whole foundation of the MicroTAS conference rests. Malmö Conference Agency is greatly acknowledged and I would especially like to thank, Lars Nilsson, Anna Martinsson and Niklas Swedenborg for their excellent and hard work in making all the necessary practical arrangements come to fruition. I would like to express my deepest gratitude to Johan Nilsson and Jörg Kutter, without whom, the administration would have been a total disaster, and for their expedient and fluent processing of all protocols and endless abstract and proceedings databases.

Last but not least, I thank all of you in the μTAS-science community for compiling and contributing your cutting-edge research for these two proceeding volumes. Without you there would be no meeting!

Thomas Laurell
μTAS 2004 Chairman
July 14, 2004

Programme Committee

Thomas Laurell
(Conference Chairman)
Lund University

Jörg P. Kutter
(Conference Co-chairman)
Technical University of Denmark

Yoshinobu Baba
University of Tokushima

David Beebe
University of Wisconsin - Madison

D. Jed Harrison
University of Alberta

Klavs Jensen
Massachusetts Institute of Technology

Takehiko Kitamori
University of Tokyo

Johan Nilsson
Lund University

M. Allen Northrup
Microfluidic Systems Inc.

Shuichi Shoji
Waseda University

J. Michael Ramsey
University of North Carolina

Sabeth Verpoorte
University of Groningen

Jean Louis Viovy
Curie Institute

The Programme Committee and The Local Organising Committee kindly acknowledge the support from the following:

Gold sponsors

VINNOVA

The Crafoord Foundation

SCIENCE • TECHNOLOGY • MEDICINE

Swedish Foundation for Strategic Research

MCPT

micralyne

Silver sponsors

SAMSUNG

microplast ab®
www.microplast.se

GYROS

LUND
UNIVERSITY

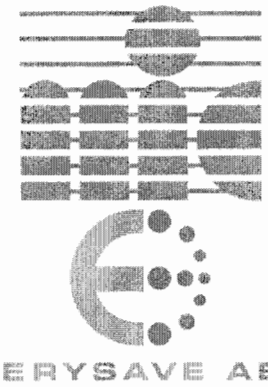

ERYSAVE AB

ATS MEDICAL

Bronze sponsors

silex MICROSYSTEMS

Johnson & Johnson

Caliper LifeSciences

mfsi MICROFLUIDIC SYSTEMS, INC.

Other support

analytical chemistry

Science AAAS

LAB ON A CHIP

www.rsc.org/loc

JOURNAL OF SEPARATION SCIENCE

Table of Contents
Volume 1

Day 1 – Monday, September 27, 2004

Plenary I

Monday Session A – Particle Sorting

Monday Session B – Motormolecules

Monday Session A – Cell Positioning

Monday Session B – MEMS

Monday Plenary II

Monday Poster Sessions – Applications I

Monday Poster Session – Microfluidics I

Monday Poster Session – Nanotechnology

Monday Poster Session – Others

Monday Session A – Fluid Pumping

Monday Session B – Proteomics

Day 2 – Tuesday, September 28, 2004

Tuesday Session A– Cell Culture I

Tuesday Session B – Nanochannels

Tuesday Session A – Particles

Tuesday Session B – Optical Detection

Tuesday Plenary IV

Tuesday Poster Session – Applications II

Tuesday Poster Session – Microfluidics II

SINGLE MOLECULE NANO-BIOSCIENCE

Toshio Yanagida

Graduate School of Frontier Bioscience and Graduate School of Medicine, Osaka University, 1-3, Yamadaoka, Suita, Osaka, 565-0871, Japan

1. Introduction

Biomolecules assemble to form molecular machines such as molecular motors, cell signal processors, DNA transcription processors and protein synthesizers to fulfill their functions. Their collaboration allows the activity of biological systems. The reactions and behaviors of molecular machines vary flexibly while responding to their surroundings. This flexibility is essential for biological organisms. The underlying mechanism of molecular machines is not as simple as that expected from analogy with man-made machines. Since molecular machines are only nanometers in size and has a flexible structure, it is very prone to thermal agitation. Furthermore, the input energy level is not much difference from average thermal energy, k_BT. Molecular machines can thus operate under the strong influence of this thermal noise, with a high efficiency of energy conversion. They would not overcome thermal noise but effectively use it for their functions. This is in sharp contrast to man-made machines that operate at energies much higher than the thermal noise. In recent years, the single molecule detection (SMD) and nano-technologies have rapidly been expanding to include a wide range of life science. The dynamic properties of biomolecules and the unique operations of molecular machines, which were previously hidden in averaged ensemble measurements, have now been unveiled. The aim of our research is to approach the engineering principle of adaptive biological system by uncovering the unique operation of biological molecular machines. I survey our SMD experiments designed to investigate molecular motors, enzyme reactions, protein dynamics and cell signaling, and discuss the mechanism of biological molecular machines.

2. Single-molecule detection (SMD) techniques

How advantageous is SMD for investigations? Observing and manipulating biomolecules allows their dynamic behaviors to be directly revealed, as has been demonstrated for motor proteins. Reactions of biological molecules are generally stochastic. Therefore, even if the reactions of molecules are initiated at the same time, they cannot be synchronized, so the dynamic behaviors of individual molecules are averaged and hidden in ensemble-averaged measurements. *In vivo*, biomolecules work in dynamic and complicated heterogeneous systems, involving different kinds of molecules such as cell-signaling proteins. It is difficult to quantitatively detect dynamic behaviors of target molecules in such systems by ensemble-averaged measurements. The SMD techniques are expected to overcome these difficulties and have already been successfully applied to study the dynamic properties of biological molecules such as motor proteins, enzymes, RNA polymerase and cell-signaling proteins [1, 2].

The SMD techniques are based on two key technologies for single-molecule imaging and single-molecule nanomanipulation. First, the imaging technique will be explained. The size of biomolecules and even their assemblies are in the order of nanometers, so they are too small to observe by optical microscopy. To overcome this problem, biomolecules can be fluorescently labeled and visualized using fluorescence microscopy. Single fluorophores in aqueous solution were first observed in 1995 by using total internal reflection fluorescence microscopy (TIRFM) and conventional inverted fluorescence microscopy [3]. The major problem to overcome when visualizing single fluorophores in aqueous solution is the huge background noise, which can be

8th International Conference on Miniaturized Systems for Chemistry and Life Sciences
September 26–30, 2004, Malmö, Sweden

caused by Raman scattering from water molecules, incident light breaking through filters, luminescence arising from the objective lens, immersion oil and dust. In this system, the evanescent field was formed when the laser beam was totally reflected by the interface between the solution and the glass. The evanescent field was not restricted to the diffraction limit of light, thus it could be localized close to the glass surface, which resulted in the penetration depth (~150 nm) being several-fold shorter than the wavelength of light. Therefore, the illumination was restricted to fluorophores either bound to the glass surface or located close by, thereby reducing the background light. Furthermore, by careful selection of optical elements, the background noise could be reduced by 2000-fold compared with that of conventional fluorescence microscopy. This made it possible to clearly observe single fluorophores in aqueous solution. Fluorescence measurements from fluorophores attached to biomolecules and ligands allow the detection of, for example, the movements, conformational changes, enzymatic reactions and cell-signal processes of biomolecules at the single molecule level.

The second key technology is single-molecule nanomanipulation. Biomolecules and even single molecules can be captured by a glass needl[e] [5-7] or by beads trapped by optical tweezers. The optical tweezers are the tool to trap and manipulate particles of 25 nm to 25 μm in diameter by the force of laser radiation pressure. The particle is trapped near the focus of laser light when focused by a microscope objective with a high numerical aperture. The optical tweezers produce forces in the piconewton range on the particles. Biomolecules are too small to be directly trapped by the optical tweezers, so they are generally attached to an optically-trapped bead. Microneedles or a bead trapped by a laser act as a spring that expands in proportion to the applied force. Thus, the force and the displacement caused by the biomolecules can be measured. The displacement of a microneedle and a bead has been determined with a subnanometer accuracy, much less than the diffraction limit of an optical measurement. This accuracy of displacement corresponds to the sub-piconewton accuracy in the force measurements. Thus, the mechanical property of biomolecules can be determined directly at the single-molecule level. Furthermore, combined with the single-molecule imaging technique, simultaneous measurements of mechanical and chemical reactions of single biomolecules are possible.

3. Movement and ATPase turnovers of biological molecular motors

The SDM techniques were first used to study molecular motors. The example discussed here is that of a microtubule-based kinesin motor, which transports organelles along a microtubule in cells. Kinesin is composed of two heavy chains, each consisting of a force-generating globular domain (head), a long α-helical coiled-coil and a small globular C-terminal domain (tail). Microtubules are cylinders comprising parallel protofilaments, which usually number 13 or 14 when reassembled *in vitro*. Movement of single kinesin molecules along a microtubule has been directly observed by TIRFM. Kinesin molecules, fluorescently labeled at the tail-end without damage, were added to microtubules adsorbed onto a glass surface in the presence of ATP (adenosine triphosphate). This demonstrated directly that a single molecule of kinesin could processively move for long distances along a microtubule without dissociating [4].

In general, the motions of molecular motors and operations of other biomolecules are fueled by the chemical energy released from ATP hydrolysis. Kinesin and myosin are both motor proteins and ATPases. To uncover how the biomolecules work using the chemical energy from ATP, it is crucial to observe the individual cycles of ATP hydrolysis by single ATPase molecules. This has been achieved using the single-molecule imaging technique TIRFM in combination with the fluorescent ATP analog, Cy3-ATP . This method was first applied to an actin-based myosin motor that is involved in muscle contraction and other cellular motility. Myosin has a similar structure to

kinesin, although it is twofold larger in size. Cy3-ATP is hydrolyzed by myosin in the same way as ATP . The rate of the biochemical cycle of ATP hydrolysis averaged for many events or individual myosin molecules was consistent with that obtained by a conventional biochemical method using a suspension of myosin.

4. Simultaneous observation of the ATPase turnover and mechanical events of an actin-based myosin motor

To investigate how the mechanical event of myosin corresponds to the ATPase cycle, the single-molecule imaging technique was combined with optical-trapping nanometry to simultaneously measure individual ATPase cycles and mechanical events of a single myosin molecule (Fig. 1). Dissociation of the myosin head from actin corresponded to the binding of ATP, and association of the myosin head with actin and generation of displacement were followed by dissociation of a nucleotide (most likely ADP). Each displacement corresponded to a single ATP molecule [5].

Understanding the process of a displacement became essential to investigating how myosin works using the chemical energy from ATP. Optical-trapping nanometry cannot resolve this process, because the displacement is determined indirectly through a long actin filament and optically-trapped beads, which have an unknown elasticity. Thus, the signal to noise ratio is not high enough to resolve the process. To overcome this problem, a more direct method combining scanning probe and single-molecule techniques has been developed. A single myosin head was attached to the tip of a scanning probe and the process of a displacement was resolved by measuring the displacement of a scanning probe with nanometer and millisecond accuracies. The results showed that a myosin head moved along an actin filament with regular 5.5 nm steps and underwent five steps to produce a maximum displacement of 30 nm per displacement (i.e. representing the ATPase cycle). As the step size coincides with the actin monomer repeat (5.5nm) and each 5.5 nm step is not directly coupled to the ATPase cycle (loose coupling), the results strongly indicate that the myosin head walks along the actin monomer repeat using biased Brownian motion . This idea challenges the widely accepted view that the movement is caused by a large conformational change in the myosin head, tightly coupled to the ATPase cycle in a one-to-one fashion (tight coupling) [6].

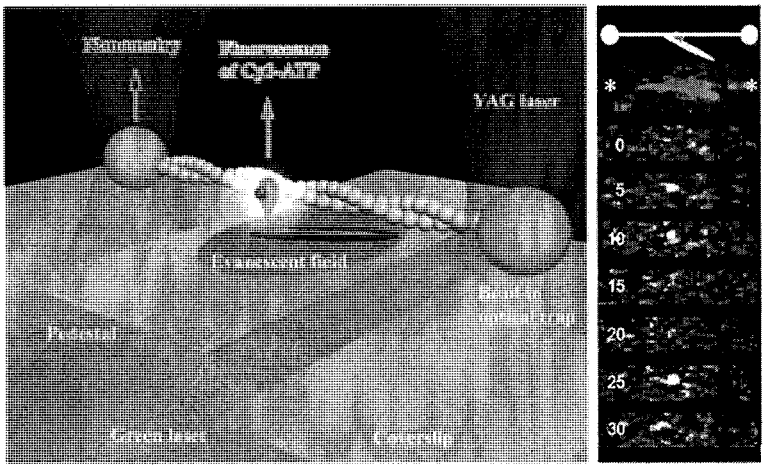

Figure 1. Single molecule imaging and optical-trapping nanometry to perform simultaneous measurements on individual ATPase cycles and mechanical events on a single myosin molecule.

5. DNA transcription

The initial steps of gene expression include the binding of RNA polymerase (RNAP) to DNA, the search for a promoter in the DNA sequence and the synthesis of RNA based on the information encoded by the DNA. These steps are central regulatory mechanisms of gene expression and have been extensively investigated. Harada *et al.* have observed single, fluorescently labeled RNAP molecules interacting with a single molecule of DNA suspended in solution using optical traps. The kinetic studies have proposed some mechanisms for promoter searching based on the results of the binding of RNAP molecules to specific and nonspecific sites on the DNA: sliding, intersegment transfer and simple dissociation and/or association reactions. This observation provides direct evidence that a sliding motion is a mechanism used for the search of promoters . The association and dissociation rate constants of RNAP could be also determined, depending on the sequence of DNA and on the mechanical strain exerted on the DNA. These values proved difficult to determine in solution because DNA molecules aggregate to form a network structure. The transcription process was directly monitored by measuring the displacement or rotation of DNA during the interaction with RNAP by manipulating DNA with optical and magnetic tweezers. One end of DNA is attached to a magnetically-trapped bead and the other is interacting with a RNAP adsorbed onto the glass surface. Rotation of DNA is determined by monitoring the rotation of the bead. The results showed that the rotation rate is consistent with high-fidelity tracking. The rotation per base pair is as much as 35□ and should, in principle, be detectable. Therefore, this method could resolve individual steps of transcription in real time [7].

6. Future perspectives

Recently, life science has made remarkable progress. This progress has been possible because of the identification of functional proteins and studies on the characteristic (structural and functional) properties of proteins as revealed by molecular cell biology, structural biology and molecular genetic approaches. The DNA sequences of not only invertebrates but also of vertebrates (including human) are now available. Thus, research is charging into the post-genomic era. In this era, we tend to emphasize the concept that the structure explains the function and we endeavor to understand the mechanisms of the proteins and molecular machines based on this concept. However, knowing the function of proteins and molecular machines is not a simple task. Moreover, we could not understand the function of these proteins even if we knew their structures. Proteins and molecular machines are not simple and their function cannot be learned in analogy to artificial machines. Proteins and molecular machines have a size in the nanometer range, and a dynamic and soft structure. In addition, the input energy to the molecular machines is comparable to thermal energy. Molecular machines function at a very high efficiency when exposed to thermal agitation. This is contrasted by artificial machines, which use much higher energy than thermal energy to work rapidly, accurately and deterministically. For such reasons, it is necessary to understand the dynamic properties of proteins themselves and their interactions to each other. The SMD techniques have been developed as techniques to directly monitor the dynamics of proteins and molecular machines and have rapidly expanded to include a wide field of biological sciences. Combined with nanotechnology from the engineering field, the SMD techniques will prove more powerful in the future. Thus, the SMD will govern and lead the future direction for research in proteins and molecular machines.

References

[1] A. Ishijima and T. Yanagida Single Molecule Nano-Bioscience. *Trends in Biochemical Sciences*, 26, 438-444 (2001)
[2] Y. Sako and T. YanagidaSingle-molecule visualization in cell biology. *Nature Review Cell Biol.* ss1-ss4 (2004)
[3] Funatsu, T. et al. Imaging of single fluorescent molecules and individual ATP turnovers by single myosin molecules in aqueous solution. *Nature* 374, 555–559 (1995)
[4] Vale, R.D. et al. Direct observation of single kinesin molecules moving along microtubules. *Nature* 380, 451–453 (1996)
[5] Ishijima, A. et al. Simultaneous measurement of chemical and mechanical reactions. *Cell* 92, 161–171 (1998)
[6] Kitamura, K. et al. A single myosin head moves along an actin filament with regular steps of 5.3 nanometres. *Nature* 397, 129–134 (1999)
[7] Harada, Y. et al. Direct observation of DNA rotation during transcription by E. coli. RNA polymerase. *Nature* 409, 113–115 (2000)

HIGH-SPEED PARTICLE SORTING: COMBINING DIELECTROPHORESIS AND FLUID FLOW

David Holmes, Mairi E. Sandison, Nicolas G. Green and Hywel Morgan
School of Electronics and Computing Science,
University of Southampton, Highfield, Southampton, SO17 1BJ, UK.

Abstract

We present a high-speed particle sorting and deflection system which is an integral part of a micro flow-cytometer chip capable of high speed detection and sorting of micron-sized particles. The device sorts particles using a combination of DEP and hydrodynamic forces. DEP focusing of particles is used to axially centre particles in a channel. Negative dielectrophoresis, together with hydrodynamic flow is used to achieve high speed particle sorting at a microfluidic T-junction.

Keywords: particle sorting, dielectrophoresis, AC-electrokinetics, micro-flow cytometry

1. Introduction

A number of particle sorting and detection devices have appeared in the μTAS literature in recent years [e.g.1-6]. Many of these devices mimic the operating principle of a bench-top flow-cytometer but on the micro-scale. Flow cytometers (or Fluorescent Activated Cell Sorters, FACS) allow counting and sorting of micron-sized particles such as cells and latex beads. The disadvantages of conventional FACS machines are the requirement for relatively large sample volumes (100μl), skilled operators and the high cost of such systems. Many of the functionalities of a FACS machine have been implemented into micro devices such as detection of fluorescence [1, 2], or scattering from particles [4]. Impedance detection has also been incorporated into micro-devices for single cell analysis [5]. Although particles can be counted at relatively high speed in these micro-devices, particle sorting speeds are generally lower.

In this paper we present a novel approach to achieve rapid particle sorting. The method uses a combination of hydrodynamic forces and dielectrophoresis to achieve high speed particle deflection and sorting. Fuhr and co-workers [6] presented DEP based cell sorting devices which used bar-shaped electrodes that deflected particles across a channel to one or other of an outlet. This method is relatively slow as the particle may have to be moved a relatively large distance across the channel to the outlet. Our device differs from previous designs in that it uses a particle positioning system to focus particles into the centre of the channel prior to the sorting junction as shown in Fig. 1. The operating principle of the device is shown in Fig. 2. Particles are centred along the axis of the channel, and arrive at the T-junction with equal probability of flowing into either outlet. A small negative-DEP deflection force is provided by the electric field configuration of the three electrodes at the gate, pushing a particle from the central stream line, so that it passes into one or other of the outlets.

2. Fabrication

Electrodes were patterned using photolithography on 500 μm thick glass substrates. Si_3N_4 insulator was deposited to all but the tips of the electrodes, a polyimide flow channel was fabricated and a second set of electrodes was aligned and bonded to form the lid. The main channel has dimensions of 40μm high and 80 μm wide, with both outlets of equal dimensions, 40μm high and 40 μm wide. Inlet and outlet holes were drilled in the lid for sample entry and exit, which was performed using pressure driven flow via an external pump. A schematic diagram and SEM of one half of the device is shown in Fig. 1.

3. Results and discussion

The initial set of focusing electrodes pushes particles into a tight axially centered beam using negative [7, 8]. This ensures that all the particles follow the same trajectory along the main channel, with the same velocity, equal to the maximum flow rate in the device. An AC voltage is applied to the sorting electrode as shown in Fig. 2, to deflect individual particles away from the equilibrium position into one of the two outlets. With a voltage of 20V peak-peak at 1MHz it was possible to deflect 6μm diameter latex beads (Molecular Probes) with velocities of $1500\mu ms^{-1}$. At this velocity the system could sort particles at a rate of 200-300 per second.

Fig. 3 shows consecutive frames taken from a video showing the tracks of individual beads being sorted within the device. The tracks appear stretched because the particles move several tens of microns during each video frame (40ms per frame). The top sequence shows a particle sorted to the left, the bottom sequence shows a particle being sorted into the right channel. The bright image present in all frames is due to beads which have adhered to the channel wall.

4. Conclusions

A device has been implemented that can sort particles using a combination of dielectrophoretic forces and hydrodynamic forces. Most particles readily undergo negative DEP at high frequencies, so that latex beads, cells or viruses could be sorted at high speed into different channels using relatively low AC voltages. The technology is easily scalable so that any number of Y or T-junction could be fabricated on a chip and particles gated into an array of different channels. In an extension to this work we have implemented this sorting principle into a full automated micro-FACS system, where fluorescently labelled particles are detected using confocal optics together with real-time control electronics to control the sorting. Combining DEP-based focussing and sorting with the advantages of sub-nL optical detection volume will enable the development of rapid configurable automated particle sorting systems. Sort speeds greater than 1000 particles per second are expected with improved designs.

Acknowledgements

This research is supported by the Emerging and Underpinning Technologies Domain of the UK MoD Corporate Research Programme. The authors would like to thank Dr Tim Cox for useful discussions.

References

[1] Schrum, D.P., *et al.*, Analytical Chemistry, **71** 4173-4177 (1999).
[2] McClain, M.A., *et al.*, Analytical Chemistry, **73** 5334-5338 (2001).
[3] Fu, A.Y., *et al.*, Nature Biotechnology, **17** 1109-1111 (1999).
[4] Pamme N., Koyama R. and Manz R. Lab on a Chip, **3** 187–192 (2003).
[5] Gawad, S., Schild L. and Renaud P., Lab on a Chip, **1** 76-82 (2001).
[6] Fiedler, S., *et al.*, Analytical Chemistry, **70** 1909-1915 (1998).
[7] Morgan, H., Holmes, D., Green, N. IEE Proc. Nanobiotechnology, **150** 76-81 (2003).
[8] Morgan H., Holmes D. and Green N. in "Electrostatics 2003" edt. H. Morgan, IoP Publications, 119-124 (2003).

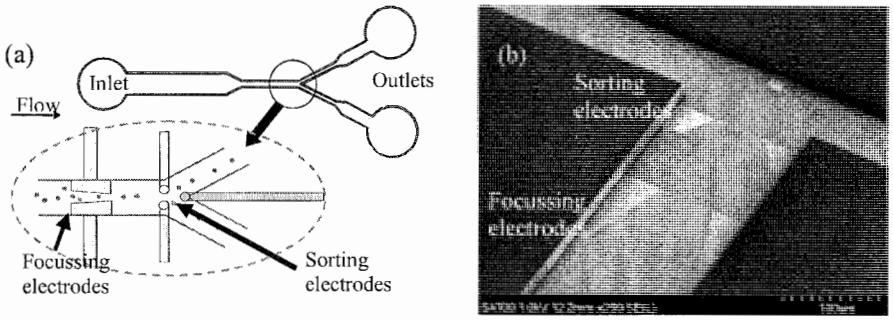

Figure 1. (a) Schematic diagram of the sorting device together with an SEM of the electrodes (b)

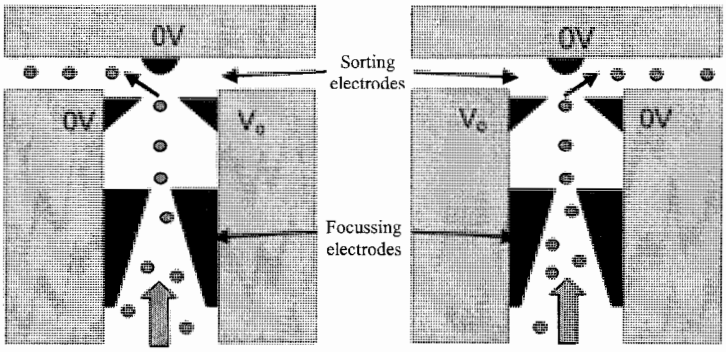

Figure 2. Diagram showing the operating principle of the sorting chip, together with the focusing and sorting electrodes. Particles are focused into a narrow beam along the axis of the channel. The combination of DEP and hydrodynamic forces at the sorting junction move particles left or right according to the voltage sequence applied to the three sorting electrodes.

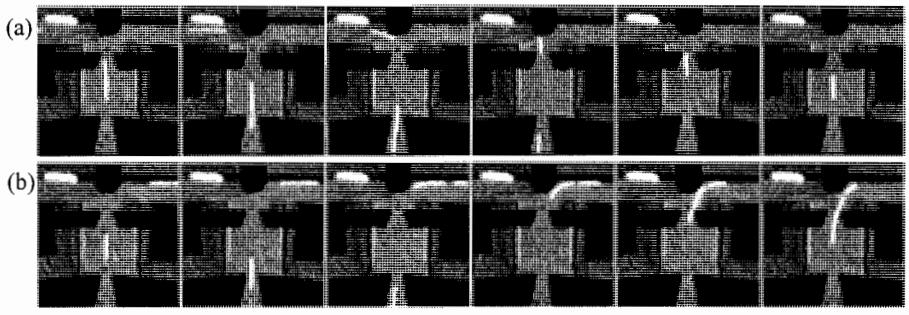

Figure 3. Successive sequence video images (40ms time interval) showing particle trajectories in the chip. In (a) a particles are sorted to the left, whilst in (b) particles are sorted to the right. The particles appear elongated because they move a considerable distance in a single video frame. V_o = 20Vpp at 1MHz.

CONTINUOUS PARTICLE SEPARATOR BASED ON PERIODICAL DEP ELEMENTS

Stefan Kostner[1], Jeroen H. Nieuwenhuis[1], Edeltraud Svasek[2], Peter Svasek[2], Arthur Jachimowicz[1] and Michiel J. Vellekoop[1]

[1]*Institute of Sensor and Actuator systems (ISAS), Vienna University of Technology, Gusshausstrasse 27-29, A-1040 Vienna, Austria*

[2]*Ludwig Boltzmann Institute of Biomedical Microtechnology, Vienna, Austria*

Abstract

In this work a novel device for continuous separation of particles based on dielectrophoresis (DEP) is presented. The dependency of the dielectrophoretic effect on the particle radius is exploited to separate particles of different size in a microfluidic channel. In the device a separation is established by forcing the particles on trajectories of different mean velocity in a parabolic flow profile of a pressure driven flow.

Keywords: dielectrophoresis, particles, separator

1. Introduction

We present a continuous particle separator using periodical dielectrophoresis (DEP) elements (Fig. 1). Dielectrophoresis is the effect that a polarizable particle experiences a force when exposed to a non-uniform electric field. As the particles flow through the separation channel, dielectrophoretic forces are applied to move them up and down, which results in trajectories as shown in Fig. 2. The amplitude of this trajectory strongly depends on the particle size. Since the velocity profile of the liquid in a pressure driven flow is parabolic, the flow-speed of a particle depends on its vertical position in the channel. Larger particles (for which the amplitude of the trajectory is larger) will now have a lower average velocity, which results in longer retention time than smaller particles. At the end of the channel there will be a separation of particles depending on their diameter. This device does not use gravity as a parameter for separation, as in other devices e.g. [1].

2. Theory

For the description of the particle behavior dielectrophoretic and hydrodynamic forces are taken into account. Using a dipole approximation for a polarized particle in an electric field and utilizing the so-called Stokes Approximation for the hydrodynamic drag, the forces acting on a particle read:

$$F_{DEP} = 2\pi\varepsilon_l R^3 K \nabla E_0^2$$

$$F_{DRAG} = 6\pi\eta R(v_l - v_p)$$

where $K = (\varepsilon_p - \varepsilon_l)/(\varepsilon_p + 2\varepsilon_l)$ is the so-called *Clausius-Mossotti Factor* and ε_l and ε_p are the permittivities of liquid and particle respectively. R is the particle radius, E_0 is the local electric field, η is the viscosity of the liquid and $(v_l - v_p)$ is the difference of liquid and particle velocity. The equilibrium between these expressions and the inertia force $F_I = m_p dv_p / dt$ as well as the buoyancy force is used in a model to determine the trajectory of a particle in a channel of given electric and flow field distribution.

3. Device

The device consists of two glass slices bonded together with SU-8 [2], which also defines the channel dimensions. The liquid connections are defined by through holes in one of the glass wafers. The DEP electrodes (Cr/Au) are 80μm wide.

A simple particle trap structure was used to accumulate and periodically release the particles, allowing for continuous operation of the device. So, both sample injection and separation are controlled electronically.

A dynamic simulation model has been developed to optimize the electrode structure and to estimate the voltage necessary for trapping the particles. The force equilibrium between dielectrophoretic-, drag- and inertial forces is calculated from which the particle trajectory and retention time is determined (Fig. 2). The difference in retention time is a measure for the separation efficiency.

The separation channel has a periodic electrode structure to generate strong non-uniform electric fields. Because the electrodes are applied on both top and bottom the particles are forced to follow a trajectory moving up and down periodically in the channel, minimizing the influence of gravity (Fig. 2).

4. Results and discussion

Polystyrene particles of 8 and 15 μm diameter suspended in de-ionised water were pumped through the device using a syringe pump. For the characterization of the device the retention time of these particles was measured separately using a manually triggered stopwatch computer program.

At a DEP voltage of 5.5 V (RMS, 1 MHz) the larger particles show an average 25% longer retention time than the smaller particles, which proofs the concept. A histogram for several measurements is shown in Fig. 4. The results presented in this paper can be assumed to contain an error caused by the reaction time of the manual trigger process (estimated error ± 0.1s). Therefore, the measurements are expected to show an even better distribution if a fully electronic (and more accurate) detection would be applied.

Additional measurements were carried out using a particle sample mix containing 8 and 15μm particles. Using a similar stopwatch program as mentioned above the time between release and arrival of the first small and the first large particle was recorded. These measurements confirm the results shown in Fig. 4.

In addition to separation of particles based on their size, our setup also permits separation on the basis of dielectric constant and electrical conductivity. This topic is part of current investigations.

5. Conclusions

We have simulated, designed and fabricated a novel particle separation device based on periodic DEP elements. Our first measurements demonstrate that particles of 8 and 15μm show significant differences in retention time (25%) at a DEP voltage of 5.5 V (RMS, 1 MHz).

References

[1] H. Sano, H. Kabata, O. Kurosawa, M. Washizu, "Dielectrophoretic chromatography with cross-flow injection", The Fifteenth IEEE International Conference on Micro Electro Mechanical Systems, 2002, 20-24 Jan. 2002, pp. 11-14

[2] P. Svasek, E. Svasek, B. Lendl, M.J. Vellekoop, "SU-8-Based Fluidic Devices", proc. of Eurosensors XVII, September 21-24, 2003, Guimaraes, Portugal, 2003, pp. 283-286

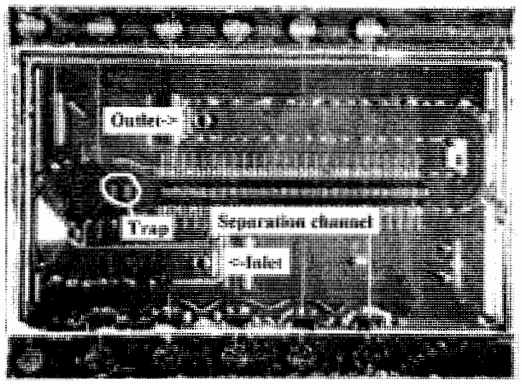

Figure 1. Particle separation chip (1.5x2cm²). Channel height 70µm, width 1mm, length 10.4 mm. The separation channel has 26 DEP elements.

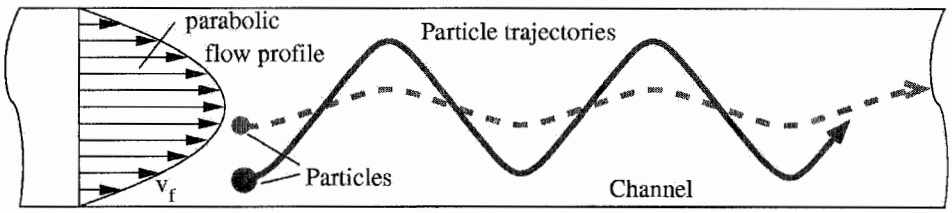

Figure 2. Operation principle of the separation channel. Hydrodynamic drag moves the particles in horizontal direction while DEP forces move them up and down. The dependency of the trajectory amplitude on the particle size is exploited to establish a separation.

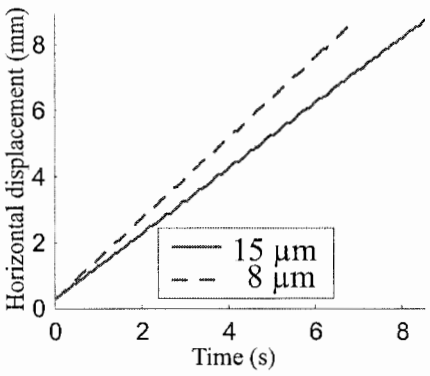

Figure 3. Simulation results for the horizontal displacement of 8 and 15µm particles.

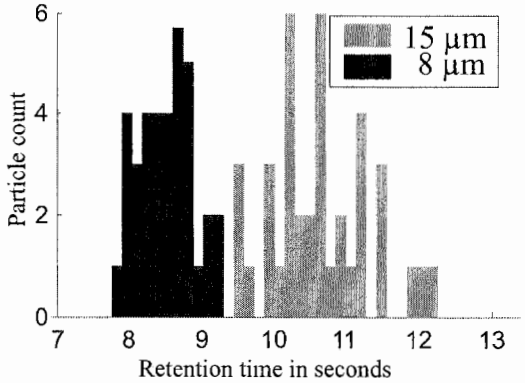

Figure 4. Histogram of retention time measurements for different particle sizes. 15µm particles show an average 25% longer retention time.

STUDY OF HIGH SPEED ACOUSTIC SEPARATION IN MICRO-CHANNELS USING μ-PIV

Holden Li, Vipin Vitikkate, Thomas W. Kenny
Department of Mechanical Engineering, Stanford University, Stanford, California 94305, USA

Abstract

In this paper, we report the behavior of suspended particles comparable to human blood cells under the influence of an ultrasonic acoustic field, using micron-resolution particle image velocimetry (μ-PIV). This work is in progress towards the design of an integrated micro-channel structure for cell separation in the microscale regime. The acoustic separation method directly differentiates particles based on their size at low power (less than 100 mW) and with small sample sizes (tens of micro-liters). Experimental results show that particles of different sizes can be separated by a careful design of a continuous flow micro-channels system. We have demonstrated the capability of separating over a million particles in less than 5 minutes.

Keywords: acoustic separation, particle image velocimetry, micro-channels, μ-TAS

1. Introduction

Centrifuges are typically used to separate various components of the whole blood in laboratories. This method has proven to be fast and effective in large-scale operation, with an acceleration field up to 10,000G. But the dependence of the radius of rotation prevents further miniaturizing a centrifuge into a micro-scale device. In order to realize a μ-TAS that can diagnose human health with low power consumption and low sample size, a robust and high speed separation mechanism is desired. Various other methods of micro-separation on cells have also been proposed over the years, like micro-filtration [1], magnetic separation [2], electrophoresis [3], di-electrophoresis etc. Each of these methods has its own merits and disadvantages when miniaturized to the micro-scale.

In this paper, we revisit an old technology [4] of using ultrasonic standing waves to separate different sizes of particles. The particles are concentrated at the pressure nodes of a static acoustic field based on size, density and compressibility contrast with the surrounding medium. This separation mechanism has already been proven to be effective and fast [5, 6]. However, acoustic separations often required large apparatuses with characteristic dimensions of at least centimeters and only separations of particles from the medium were demonstrated, but particles of different properties were not differentiated. There has been recent interest of repeating this method in micro-channels with diameter of less than 1mm and for separation of particles based on their densities [7].

μ-PIV is useful for understanding the behavior of different particles under the influence of acoustic pressure field and have been used in these studies to extract quantitative measurements.

2. Theory

Two dominant forces act on the suspended particles when subjected to an acoustic pressure field, namely the acoustic force and Stokes drag (ignoring diffusion, Brownian displacement and gravity which would only come into play if the acoustic field was orthogonal to them). With continuous flow in the micro-channels, the particles also experience advective forces due to the motion of the bulk liquid that carries them along. Yoshioka et al [8] proposed that the acoustic force, F_{us}, acting on a spherical particle is

$$F_{us} = \left(\frac{P_o^2 V_p \beta_f \pi}{2\lambda} \right) \left(\frac{(5\rho_p - 2\rho_f)}{(2\rho_p + \rho_f)} - \frac{\beta_p}{\beta_f} \right) \sin\left(\frac{4\pi y}{\lambda} \right) \quad (1)$$

where P_0 is the acoustic pressure, V_p is the volume of the particle, ρ_f, ρ_p, β_f and β_p represent the density and compressibility of fluid and particles respectively. The wavelength is represented by λ and y is the displacement of the particle in the pressure field.

At any instant, the acoustic force is balanced by the drag force in Equation 1, and this allows us to use velocity measurements to extract the acoustic force as a function of position. Based on this model, particles with dimensions comparable to the white blood cells (10 μm in diameter) will be concentrated on the pressure nodes about six times faster than particles comparable to a red blood cell (4 μm in diameter). We will utilize this temporal contrast to separate particles by size.

3. Experimental Setup

To understand the forces acting on particles (polystyrene beads from Duke Scientific), μ-PIV [9] is used to obtain measurements of the velocity fields. The experimental setup includes the epi-fluorescent microscope (Olympus), camera system (COHU), image capturing DAQ card (National Instrument), LabView program and Matlab software for cross-correlation calculations. For investigating the two particles separation, image capture with one wavelength is not enough. A special epi-fluorescent microscope (Carl Zeiss Axioscop 2) is used to simultaneously capture both particles, which fluoresce at different wavelengths.

4. Results and discussion

The experiments investigate the effects of varying particle size, acoustic pressure and bulk flow rate in the micro-channels. The particles range in diameter from 3 to 10 μm and the PZT voltage that provides the acoustic pressure, operating from 18 to 48 V at a frequency of 3 MHz. The flow rate is varied from 0.5 to 3 μl/min from an external pump. Based on the μ-PIV experimental results, the velocity profile of the particles due to the ultrasonic acoustic standing waves is obtained as shown in Figure 1. Particles further away from the pressure node have higher velocities than those near the nodes. It also has demonstrated that by increasing the particle sizes would lead to an increase in the acoustic force on the particles as shown in Figure 2.

The next set of experiments involves the design of this separation mechanism based on a chosen acoustic frequency, operating acoustic pressure and flow rate. By adjusting the parameters, meandering angles and flow rate of the micro-channels geometry, this experiment has shown that bigger particles are concentrated in the central stream and separated from smaller ones (Figure 3).

5. Conclusions

We have demonstrated the ability to separate different size particles with similar mechanical properties using ultrasonic standing waves. Velocity measurements are obtained with μ-PIV to shed light on the forces acting on the particles under acoustic pressure field. Future work will emphasize further miniaturization and integration within a handheld instrument.

6. Acknowledgement

We thank Stanford Center for Integrated System for sponsoring this project and Professor Juan Santiago of Stanford Microfluidics Lab for the guidance and support on the μ-PIV.

References

[1] T. Ujiie, et al, "Microfabricated separator and manipulator of blood cells for health care", Microprocesses and Nanotechnology Conference, 2000, pp. 28–29.

[2] K. Han, et al, "Paramagnetic capture mode magnetophoretic microseparator for blood cells', Hilton Head 2004, pp. 103-104.

[3] T. Ichiki, et al, "Microfabricated separator and manipulator of blood cells for health care devices", Microprocesses and Nanotechnology Conference, 2001, pp 190-191

[4] U.S. Patent US2215484, 1940.

[5] M. Saito, et al, "Ultrasonic manipulation of locomotive microorganisms and evaluation of their activity", Journal of Applied Physics Vol 92(12) pp. 7581-7586. 2002

[6] C.Lee, et al, "Low voltage high-speed ultrasonic chromatography for microfluidic assays", Hilton Head 2002

[7] F. Petersson, et al, "Particle Flow Switch Utilizing Ultrasonic in Microfluidic Channels", Micro TAS 2003
[8] K. Yoshioka, et al, "Acoustic radiation pressure on a compressible sphere", Acustica 5, 1955
[9] C. Meinhart, et al, "A PIV Algorithm for Estimating Time-Averaged Velocity Fields." Experiments in Fluids, Vol. 25, Iss. 4, pp. 316-319

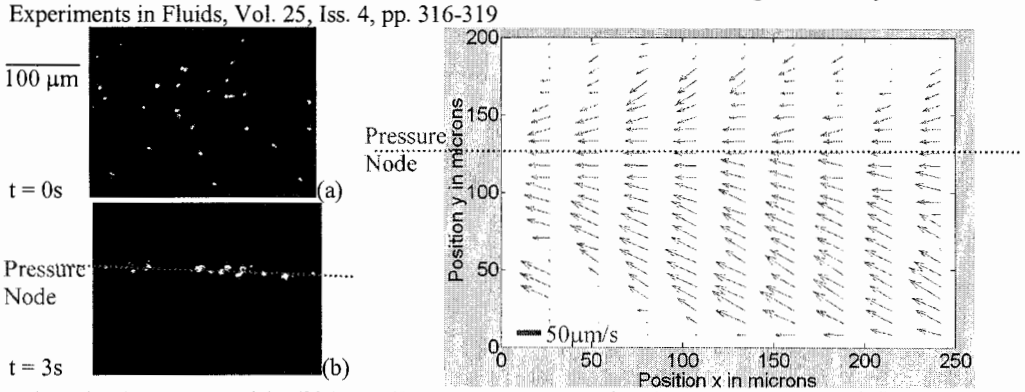

Figure 1: Fluorescent particles (20X magnification) are concentrated on the pressure node under influence of acoustic pressure at 3MHz. Pixel array is 656 by 492. 7 µm diameter particles are first randomly distributed and moved in the channel with a bulk flow rate of 1 µl/min. Particle velocity field of a region of the image is plotted on the right. Location of pressure node is represented with a dotted line.

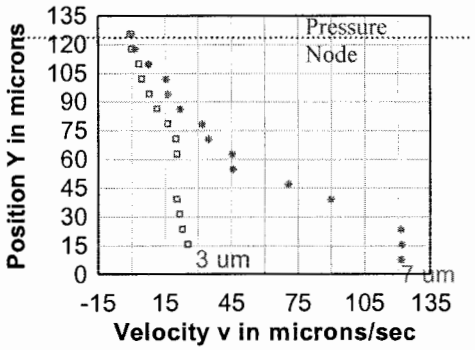

Figure 2: Plot of velocity in the y-direction versus distance across the micro-channel obtained from µ-PIV measurement of 3 and 7 µm size particles at 48V applied to the PZT at 3MHz with a bulk flow rate of 1ul/min. [Note: The velocity is obtained from the velocity field plot from µ-PIV and it has discounted the advective flow in the micro-channels.]

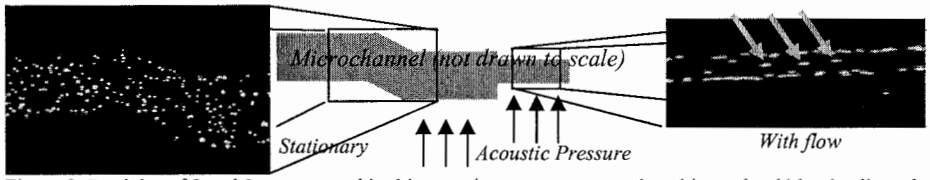

Figure 3: Particles of 8 and 3 µm are used in this experiment to represent the white and red blood cells under epi-fluorescence microscopy with 5X magnification. The flow rate is set at 3 ul/min and the ultrasonic acoustic frequency is running at 3.3MHz. Particles are mixed randomly upstream as shown in the left picture (which was taken at zero flow rate). Larger particles (pointed by arrows) are concentrated in the middle of the micro-channels and separated from the smaller ones further downstream. The oblong shapes of particles are due to streaking effects due to limitations of camera system. Fewer 8 µm particles are present in the solution since white blood cells make up only a small fraction of the whole blood.

UNIDIRECTIONAL TRANSPORTATION OF NANO BEADS BY KINESIN ON MICROTUBULES WELL-ORIENTED IN A MICRO CHANNEL

Ryuji Yokokawa[1], Shoji Takeuchi[1], Takahide Kon[2], Masaya Nishiura[2], Kazuo Sutoh[2], Hiroyuki Fujita[1]

[1]CIRMM/IIS, The University of Tokyo, 4-6-1, Komaba, Meguro, Tokyo 153-8505, Japan
[2]Graduate School of Arts and Sciecnces, The University of Tokyo, 3-8-1, Komaba, Meguro, Tokyo 153-8902, Japan

Abstract

Microtubules were immobilized inside a microfluidic channel chemically with the plus end oriented to one direction. We have also succeeded to transport kinesin-coated beads of 320 nm in diameter unidirectionally in the channel.

Keywords: kinesin, microtubule, orientation, hybrid nano transport system, biomolecular linear motors

1. Introduction

Inspired by vesicle transport in a biological cell, we aim to build a bio hybrid nano transport system based on biomolecular linear motors which enable the manipulation of micro/nano structures without fluid flow or electrokinetic force [1]. A kinesin, a motor molecule, transports an object from the minus end to the plus end of a microtubule by hydrolyzing adenosine 5'-triphosphate (ATP). In order to realize the unidirectional transport using molecules, microtubules that serve as rail molecules must be functionally oriented in the designated direction.

Some biology groups have already published on orientation techniques of microtubules [2-4]; those describe orientation method and some experimental results. However, the quantitative analysis of the technique from the engineering point of view was not performed because they focus on biological interests. Here we measure the orientation yield quantitatively in order to optimize the process condition for the unidirectional conveyance of micro/nano objects.

2. Experimental

We prepared a channel (width: 2 mm, depth: 107 μm, length: 40 mm) with two coverslips to establish the orientation process, because the process can be visualized by a dark-field microscope in millimeter-scale. The coverslip was bonded with another glass plate using double-sided adhesive tape as spacers (Fig. 1(1-3)). Fig. 1(a) shows the actual device. The outlet was connected to a syringe pump to generate a steady flow, which contribute to the easy buffer replacement in a channel even when the channel is on a microscope stage as shown in Fig. 1(b). The channel can be miniaturized down to micrometer-scale (width: 500 μm, depth: 20 μm, length: 30 mm) by the wet etching of a slide glass with

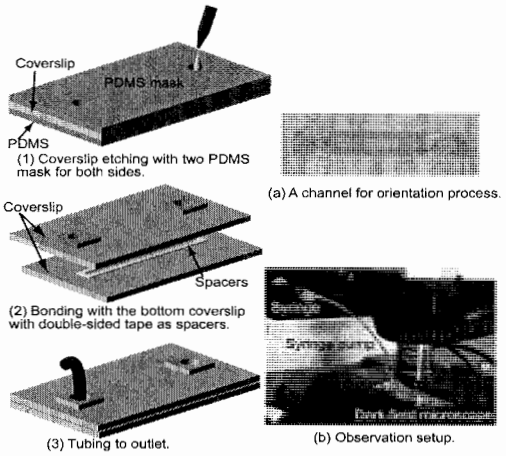

Figure 1. Fabrication process of a glass channel for the orientation test.

a PDMS mask instead of using spacers [5].

3. The orientation process

We have utilized the gliding assay in a buffer flow to orient microtubules with some modifications from [4]. Fig. 2(1) shows the direction of a buffer flow in a channel during the orientation process. Figs. 2(2) to (6) are close-up illustrations of the channel surface. The movement of microtubules is shown by arrows of which heads correspond to the minus end of microtubules. The fluid force orients microtubules parallel along the flow on a kinesin-coated surface, but the functional orientation of the plus/minus polarity cannot be realized as shown in Fig. 2(2). The pulse injection of ATP (1 mM) induces random movement of microtubules as called gliding assay (Fig. 2(3)), but the continuous flow removes microtubules gliding upstream, while almost all the microtubules gliding downstream remained on the kinesin-coated glass surface (Fig. 2(4)). Microtubules in this step were visualized by the dark-field microscope in Fig. 3(a). Buffers including 0.1 % glutaraldehyde and 0.1 M glycine are injected with intervals for incubation in order to fix oriented microtubules (Fig. 2(5)). Oriented and immobilized microtubules are shown in Fig. 3(b). After washing out chemicals, kinesin-coated beads are injected in the channel and trapped on microtubules. Injection of ATP starts bead transportation. When the plus end and the minus end of microtubules are placed upstream and downstream, respectively, beads move upstream unidirectionally (Fig. 2(6)).

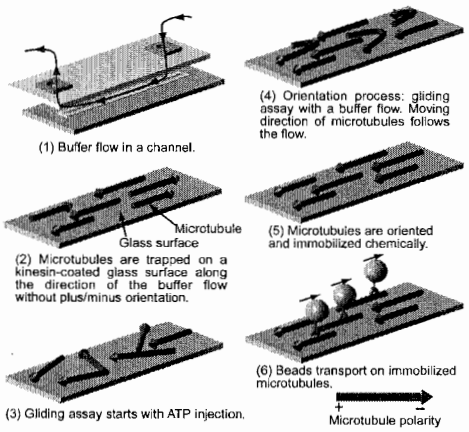

Figure 2. The orientation methodology of microtubules by a buffer flow. An arrow indicates a moving microtubule at gliding assay, which means the arrowhead is the minus end of the microtubule.

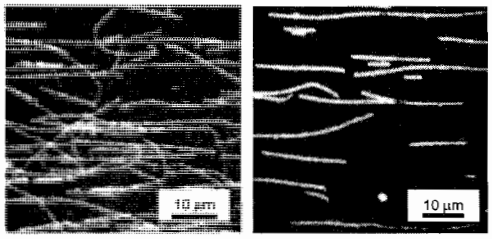

Figure 3. Microtubules on kinesin coated surface (a) during and (b) after the orientation process.

4. Results and discussion

The bead movement was captured by a differential interference contrast microscope as shown in Fig. 4(a). Fig. 4(b) is a superposition of 10 pictures with 2-second intervals between shots to visualize the unidirectional movement of beads. Fig. 4(c), an expansion of the framed area in (b), clearly shows that beads are unidirectionally transported to the right-hand side. We have investigated the relationship between the orientation yield and the buffer flow rate (Fig. 5(a)). The ratio of beads moving upstream to all the moving beads is defined as the orientation ratio to evaluate how microtubules are functionally oriented. As a control experiment the ratio of 50.3 % was measured on the physically aligned microtubules, which means beads were equally transported bidirectionally. The ratio reached about 95 % over the flow rate of 8 µm/s. The relationship between the flow rate and the density of microtubules immobilized on a glass surface is shown in

Fig. 5(b). The higher flow rate increases the orientation ratio but decreases the microtubule density. The flow rate of 8 μm/s is the best both for the orientation and the microtubule density due to their trade-off. Another important factor was the concentration of kinesin in a buffer to coat the glass surface with kinesin molecules. The lower concentration of 4 μg/ml did not yield enough microtubule density, because the flow removed almost all the microtubules. The concentration of 40 μg/ml brought tight binding between microtubules and kinesin during the orientation process. The orientation ratio was also successfully measured as 95.1 % in the micrometer-scale glass channel.

5. Conclusion

We have optimized the buffer flow rate and the protein concentration to realize the unidirectional transport of kinesin-coated beads in the millimeter-scale channel. Based on these results microtubules were also oriented in the micrometer-scale channel in which 95.1 % of moving beads moved to the designated direction. Multiple channels coated with oriented microtubules will be integrated to realize 2-D transport by kinesin motors.

References

[1] R. Yokokawa *et al.*, J. Microelectromech. Syst., to be published

[2] Y. Hiratsuka *et al.*, Biophys. J. **81**, 1555–1561 (2001)

[3] J. Clemmens *et al.*, Langmuir, **19**, 1738-1744 (2003)

[4] I. Prots *et al.*, Cell Biol. Int., **27**, 251–253 (2003)

[5] R. Yokokawa *et al.*, "Ultra-smooth Glass Channels Allowing Non-fluorescent Observation of Bio-molecules by Microscopes", μTAS2004 (2004)

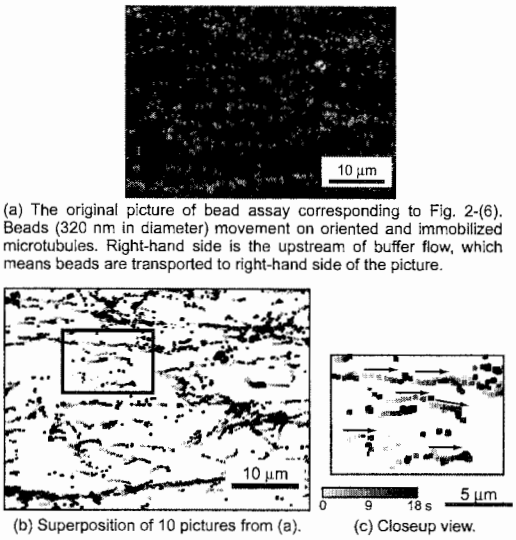

(a) The original picture of bead assay corresponding to Fig. 2-(6). Beads (320 nm in diameter) movement on oriented and immobilized microtubules. Right-hand side is the upstream of buffer flow, which means beads are transported to right-hand side of the picture.

(b) Superposition of 10 pictures from (a). (c) Closeup view.

Figure 4. Moving direction of beads.

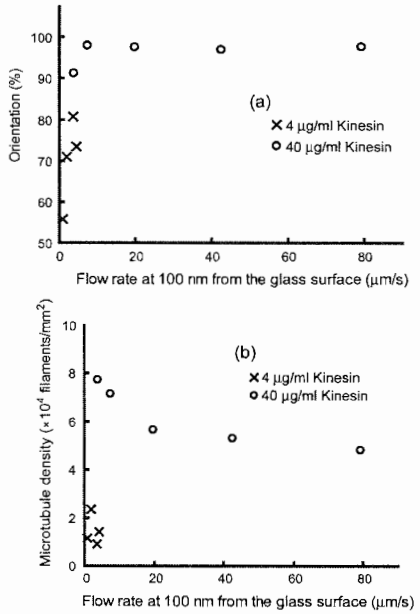

Figure 5. (a) the orientation ratio and (b) the microtubule density are measured in relation to flow rate at 100 nm from the glass surface.

NANOSCALE TRANSPORT AND ASSEMBLY WITH MOTOR PROTEINS AND MICROTUBULES

J. M. Bauer[1], A. K. Boal[2], S. B. Rivera[2], R. G. Manley[1], G. D. Bachand[2], J. Liu[3], R. P. Manginell[1], B. C. Bunker[2]

[1]*Micro Analytical Systems, Sandia National Laboratories, Albuquerque, NM, USA*
[2]*Biomolecular Materials and Interfaces, Sandia National Laboratories, Albuquerque, NM, USA*
[3]*Chemical Synthesis and Nanomaterials, Sandia National Laboratories, Albuquerque, NM, USA*

Abstract

A unique platform for the biomimetic transport of nano- and microscale materials with microtubules and motor proteins has been developed. The platform contains chemically distinct materials, fluidic and optical access on opposite sides of the platform, and the ability to incorporate electronics. The chemically distinct materials (gold and silicon dioxide) allow deposition and confinement of the biomolecular motor kinesin through selective formation of protein anti-fouling monolayers on the gold surfaces. Additionally, we have designed a custom motion-tracking program to evaluate the effectiveness of the platform in directing microtubule (and microtubule-transported cargo) motion.

Keywords: microtubules, motor proteins, motion tracking, directed transport

1. Introduction

Transport mechanisms in living systems can be used to manipulate nanoscale materials in artificial environments. For example, the movement of nanomaterials could generate macroscale changes in electrical or optical properties. With the ability to continuously manipulate materials, one could imagine applications such as reconfigurable electric or optical systems. In nature, motor proteins "walking" on microtubules transport intracellular cargoes of vesicles and genetic material. Microtubules are filament-like tubular protein structures, 25 nm in diameter with lengths between 1 and 1000 μm, depending on polymerization conditions. Hydrolysis of adenosine triphosphate (ATP) produces ordered conformational changes in motor proteins, which results in the protein walking along the length of the microtubule at the rate of approximately 1 μm/s.

Previous work has demonstrated the transport of cargo and control of microtubule motion[1,2]. We are attempting to expand these efforts and build a complete (electrical or optical) system that incorporates all of these elements. In particular, we are investigating the efficiency of various topographical features in controlling the motion of cargo-laden microtubules in microfluidic devices. A custom motion-tracking program will quantify the interaction of microtubules with the various topographical features.

Anti-fouling coatings for selective deposition of motor proteins have been used on structures fabricated from photoresist[3]. However, a noble metal surface, such as gold, is more chemically uniform than a photoresist surface and will produce a more homogeneous monolayer than is possible with photoresists. The chemical uniformity of the gold will also allow a more homogeneous mixed monolayer containing both anti-fouling and targeted binding components to selectively attach nanomaterials such as proteins and cells.

2. Platform characteristics

In our current system, microtubules glide across a silicon dioxide surface coated with kinesin motor proteins (Figures 1&2). The surface topography consists of gold features patterned on an oxide surface. The gold features have been patterned with either a lift-off technique or by coating channels etched in the substrate with gold and then milling the gold from the channel bottoms. A glass coverslip serves as the device top. The gold features are selectively coated with an anti-

fouling monolayer of alkane thiols, which prevent the kinesin from adsorbing to the gold. This surface treatment confines the microtubule motion to the oxide surface (Figure 3)[4]. A microtubule collision with a topographic feature will thus lead to a redirection of the microtubule motion.

With the fluidic and optical access on opposite sides of the platform, various solutions can be introduced and observed simultaneously. Simultaneous observation and fluidic access is particularly important in studies that involve the introduction of microtubules and/or cargo to a specific spatial location.

3. Motion-tracking program

A custom motion-tracking program has been developed to quantify the effectiveness of various topographic features in directing microtubule motion. The program measures the length, velocity, and trajectory of a number of microtubules simultaneously. A sample result of this analysis for the test case of microtubules moving in a flow cell without topographic features is shown in Figure 4. As expected, the absence of topographic features produces no preferred direction of microtubule motion. Relationships between the redirected motion and various feature geometries (such as channel width, shape, and periodicity) are currently being examined.

4. Conclusion

A unique platform for the study of microtubules and motor proteins has been presented. This platform will eventually be expanded to include mixed monolayers on the topographic features (to exclude motor protein attachment while allowing cargo attachment) and electrical connections that will be modified by the motor protein/microtubule system. Examining the motion of microtubules interacting with various platform surface features over time will yield the relative efficiencies of those features in directing microtubule and cargo motion. The results of these studies will allow optimization of system level assembly and reconfiguration of nanomaterials.

Acknowledgements

Sandia is a multiprogram laboratory operated by Sandia Corporation, a Lockheed Martin Company, for the United States Department of Energy's National Nuclear Security Administration under contract DE-AC04-94AL85000. This work was partially supported by the Division of Materials Sciences and Engineering in the Department of Energy Office of Basic Energy Sciences, Sandia's Laboratory Directed Research and Development Office, and the Defense Science Office of the Defense Advanced Research Projects Agency.

References

[1] K. J. Bohm, R. Strake, P. Muhlig, E. Unger, *Nanotechnology*, **12**, 238-244 (2001).
[2] J. Clemmens, H. Hess, J. Howard, and V. Vogel, *Langmuir*, **19**, 1738-1744 (2003).
[3] Y. Hiratsuka, T. Tada, K. Oiwa, T. Kanayama, T. Q. P. Uyeda, *Biophys. J.*, **81**, 1555-1561 (2001).
[4] A. K. Boal, J. M. Bauer, S. B. Rivera, R. G. Manley, R. P. Manginell, G. D. Bachand, and B. C. Bunker, in preparation.

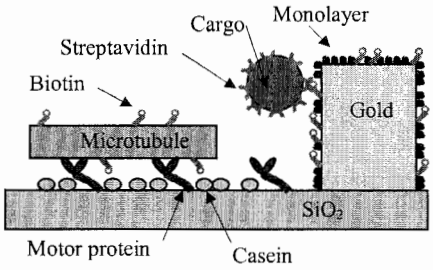

Figure 1. Schematic depicting the motion of microtubules in our microfluidic platform. Gold obstacles (which can be isolated structures or fluidic channel walls) are first coated with a monolayer to prevent motor protein absorption. Then, casein partially passivates the silicon oxide, allowing the attachment of active kinesin to the substrate. Microtubules introduced to the system will then be transported across the surface by the kinesin motor proteins. A chemical linkage, such as biotin-streptavidin, allows cargo transport.

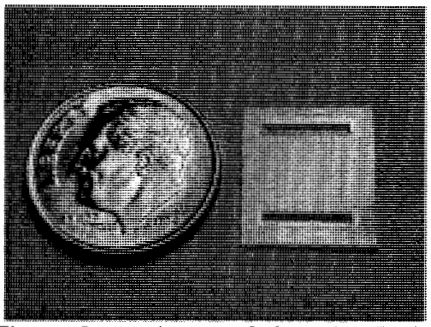

Figure 2. An image of the microfluidic platform. The through holes at the top and bottom allow fluidic access from the back and optical access from the front of the platform. For testing, the device is mounted on a coverslip.

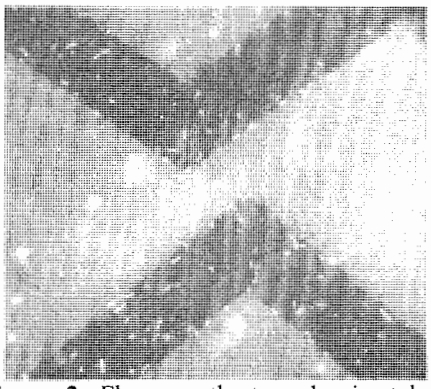

Figure 3. Fluorescently tagged microtubules confined to lithographically defined microfluidic channels by monolayers on the channel walls. Channel width = 10 μm.

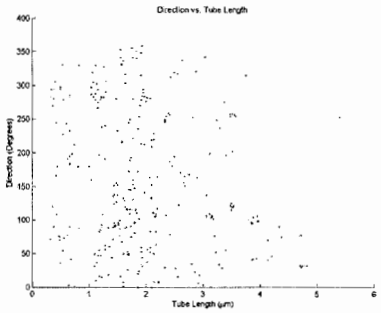

Figure 4. Microtubule direction versus tube length in a platform without topographic features. Without features to direct microtubule motion, there is not a preferred direction/orientation of motion.

WINDING UP SINGLE F_1-MOTOR PROTEIN IN FEMTOLITER CHAMBERS: THE MOLECULAR PULL-BACK CAR.

Y. Rondelez[1], G. Tresset[1], Y. Kato-Yamada[3], H. Fujita[2], S. Takeuchi[2], H. Noji[2,*].
[1] LIMMS-CNRS/IIS, [2] IIS, University of Tokyo, 153-8505 Tokyo
hnoji@iis.u-tokyo.ac.jp

Abstract

F_1 enzyme is known as the world smallest rotary motor, but its real biological function, namely the synthesis of ATP, has remained elusive. We describe the use of polydimethylsiloxane (PDMS) micrometer chamber arrays for the single molecule study of the efficiency of this molecular motor/generator. The patterned PDMS device allowed the enclosing of extremely small volumes of water solution. This packing was stable and tight. In this unprecedently small volumes (fL), activity of a unique enzyme results in rapid detectable (μM) changes in the concentration of its substrates and products. We employed this technique to follow directly for the first time the ATP consumption of F_1 as it produces mechanical work. As expected, the enzyme was found to function with a yield close to 100 %. We then turned to the ATP-generating role of F1. We attached a magnetic bead to the protein and used magnetic tweezers to force backward rotations of the enzyme. In the presence of ADP and Pi, we could detect the synthesis of ATP upon mechanical rotation at 10 Hz. As all the system was trapped in a very small volumes this ATP could not diffuse and F_1 itself served as a probe to measure the amount of produced ATP. The mechanochemical coupling was found very tight.

Keywords: Molecular motors, PDMS, Single molecule, ATP synthesis, Femtoliter.

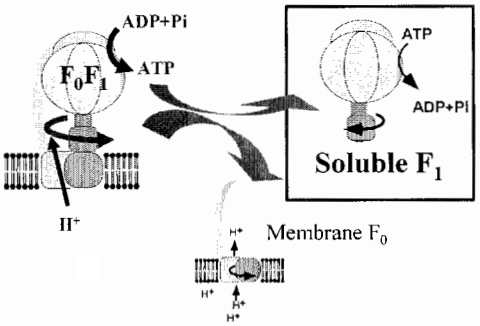

Fig. 1. F_0F_1 molecular machinery. F_0 convert the proton gradient into a mechanical torque which is transmitted to F_1. This one use the mechanical energy input to drive the synthesis of ATP against the thermodynamic potential. This process is reversible. Isolated F_1 only hydrolyse ATP to produce a mechanical torque.

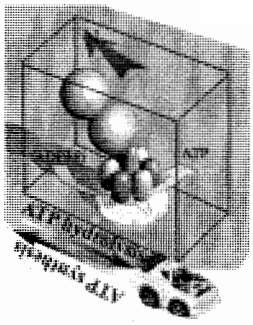

Fig. 2. A magnetic bead, fixed to F_1, allowed us to input mechanical energy through forced backward rotation. During this "pull-back" stage, ATP is produced and trapped in the femtoliter container. After release of the magnetic field, stored ATP fuels the spontaneous rotation and increases its speed.

1. Introduction

F_0F_1 enzymatic complex is responsible for the most abundant bioreaction in cells, i.e. the synthesis of ATP, the universal fuel of living organisms (Fig. 1). It is also a beautiful mechanical machinery at the nm scale [1]. It has already been demonstrated that the isolated F_1 part is able to

convert the energy released by ATP hydrolysis into a mechanical torque [2]. Since the real biological role of F_1 is not ATP hydrolysis but its synthesis from ADP and Pi, it is generally assumed that, like its electric counterparts, the enzyme functions in a highly reversible fashion, being both a motor and a generator. This last process has yet to be demonstrated quantitatively at the single molecule level [3]. We present here a microdevice approach that allowed us to observe directly the ATP-synthesis reaction under mechanical energy input to a single enzyme (Fig. 2). This experiment was achieved by the use of magnetic tweezers to mechanically rotate [4] F_1 in the backward direction, and femtoliter PDMS chambers to trap and accumulate the synthesized ATP. When the magnetic field is released, the enzyme uses this ATP to spontaneously resume its rotation in the reverse direction, at a speed that reveals the amount of produced ATP.

3. Experimental

Arrays of small cylinders were fabricated from a 1.5 μm thick SOI wafer by ICP-RIE. An aluminum layer was evaporated onto the SOI to serve as a mask for plasma etching and patterned by using 0.5 μm thick photoresist (S1805). PDMS sheets were obtained from this master which had been treated with CHF_3 plasma (100 nm thick) to facilitate the removal. The experiments were conducted in a 50 mM phosphate buffer pH=7.5, in the presence of 0.05 to 0.1 mg/mL BSA, 50 mM KCl, 2 mM $MgCl_2$. For ATP synthesis experiments 10 mM Pi and 100 μM ADP were added. Thermophilic mutant F_1 was expressed in *E. Coli*. It beared 6 His-tags on the N-Terminus of the α and β subunits and two biotins on the γ rotor part. This allowed the attachment of the protein to both the Ni-NTA modified glass slides and the streptavidin-coated plastic (or magnetic) beads. Sealing was obtained by simply pressing vertically the PDMS against the glass plate.

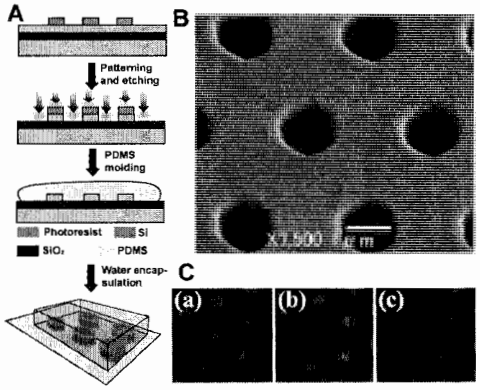

Fig. 3. (A) Microchamber arrays are fabricated in a PDMS sheet by molding from a patterned SOI wafer. (**B**) Nice features are obtained at the micrometer scale. The depth and the internal volume of the chambers shown here are 1.5 µm and 1.4 fL. (**C**) a solution containing a fluorescent dye is enclosed in the chamber (a). Then using a focused light beam, the dyes of only one chamber are bleached. (b) shows the fluorescent record just after bleaching, while (c) is taken 20 minutes later. No diffusion to the bleached chamber could be observed.

4. Results and discussion

We have designed variously sized microchambers using PDMS (Fig. 3). This polymer combines several advantages: it is soft and easy to shape, transparent to light, and doesn't interact with biological materials. We first checked the possibility to enclose durably, and without diffusion or leaks, very small volume of water in the hydrophobic chambers formed by the union of the patterned PDMS layer, and glass plate. Under the condition used, a lifetime of at least 2 hours is observed before the chambers begin to dry. When a fluorescent solution was introduced in the device, it was possible to selectively bleached the dyes in only one chamber, proving that diffusion cannot occur between neighbours containers. Under these conditions, each microchambers can be considered as an independent reaction vessel for biological studies at the femtoliter scale.

Single F_1 motors were attached onto the glass plate, grafted with a bead to allow observation and enclosed in 6 fL chamber (Fig.1). In these conditions, the enzyme quickly exhausted the small number of ATP molecules that had been trapped in the chamber and, as a consequence, its speed gradually decreased (Fig.4). The parameter for this decrease is related to k_{on}(ATP), the volume of the chamber and the coupling efficiency between ATP hydrolysis and mechanical rotation. We were thus able to confirm the high yield of this motor.

We then used the bead attached to the protein to pull backward the enzyme, that is, in the ATP-synthesizing direction. 10 Hz rotating magnetic field was applied, forcing the rotation of the bead and thus mimicking the action of the F_0 part of the full enzymatic complex. In the presence of ADP and Pi, it was expected that this mechanic energy input would drive the synthesis of ATP against chemical potentials. To detect this product, we simply released the magnetic field, allowing F_1 to resume its spontaneous rotations in the opposite direction. ATP synthesis was then recognized as an increase in the rotating speed of the enzyme during the period with no applied magnetic field (Fig.4). By comparing with a standard curve of F_1's speed build in the same condition with known concentrations of ATP, we found the coupling efficiency to be very high also for the ATP synthesizing reaction.

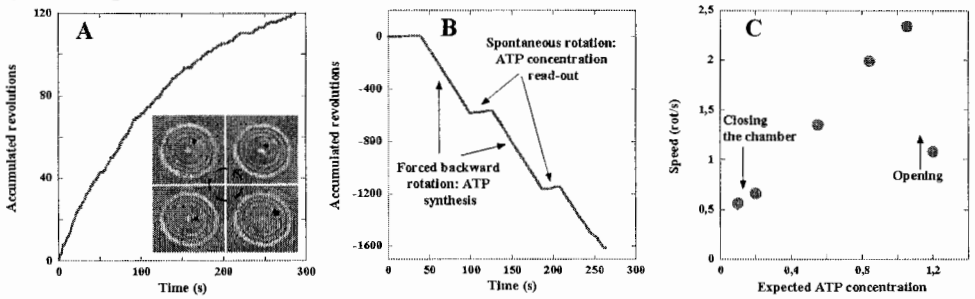

Fig. 4. (**A**) ATP molecules available inside of a 6 fl chamber are quickly exhausted by a single F_1. Decrease rate support a coupling ratio close to 100%. (**B**) Synthesis of ATP through forced backward rotation. The magnetic field is cut off from time to time to measure the spontaneous rotating speed in the motor direction. (**C**) Plot of this speed against the ATP concentration expected from the number of backward rotations shows the high efficiency of the ATP-synthesizing process.

4. Conclusion

The efficiency of the ATP synthesizing process is a very important biological value, because almost all the energy that living organism manages goes through F_0F_1. The high value we found means that this process has been finely during evolution to allow for an optimal use of available energy. Moreover the setup we present will help to reveal the succession of events that allow this uncommon mechanical-to-chemical energy transduction. In a more general sense, these arrays of small chambers allow for the first time to follow the true activity (increase/decrease in the substrate concentrations) of single enzymes. We thus expect them to find many more applications in this area.

References

[1] Boyer, P. D. *Biochim. Biophys. Acta*, **1140,** 215-250 (1993).
[2] Noji, H. Yasuda, R. Yoshida, M. Kinosita, K. Jr, *Nature*, **386**, 299-302 (1997).
[3] Itoh, H. *et al. Nature*, **427**, 465-468 (2004).
[4] Noji, H. Itoh, H. Adachi, K. Yoshida, M. Kinosita, K. Jr, *Biophys. J.* **82**, 40a (2002).
[5] Rondelez, Y. Tresset, G. Tabata, K. Nitta, H. Takeuchi, S. Noji, H. *Proc. microTAS*, 515 (2003).

POSITIONING OF CELLS IN MICROSTRUCTURE AND EXTRACTION OF CONTINUOUS DNA FIBERS FROM INDIVIDUAL CELLS

Kyohei Terao[1], Hiroyuki Kabata[2] and Masao Washizu[1]

[1]Dept. of Mechanical Engineering, The University of Tokyo, Hongo , Bunkyo-ku, Tokyo, Japan
[2]Horizontal Medical Research Organization, Kyoto University, Yoshida konoe, Sakyo-ku, Kyoto, Japan

Abstract

The paper presents two technologies for DNA fiber stretching: cell positioning and drawing DNA fibers out of the cell. The device consists of an electroosomotic flow (EOF) chamber having micro fabricated structures. The structure for cell positioning has openings whose dimension is chosen to accept only one cell at a time, to which cells carried by uni-directional EOF are positioned, one cell at each opening. After enzymatically rupturing cells, DNA fibers can be drawn out of each cell and stretched by EOF. To maintain stretched conformation, we use an array of micro-pillars around which the fiber is wound by sequentially changing the direction of EOF. The fiber is freely suspended without contact to solid surfaces except at the pillars, allowing free access of foreign molecules. Such configuration is expected to realize high-efficiency gene location based on DNA hybridization or protein binding.

Keywords: electroosmotic flow, DNA fiber, FISH, cell, manipulation

1. Introduction

Stretching of continuous DNA fibers is the basic technique in gene location based on observation of molecular binding, including extended-fiber FISH (Fluorescence *in situ* Hybridization) [1]. The requirement is to stretch continuous long DNA strand, typically more than 1 Mega base-pairs, in such a way to allow binding of foreign molecules (fluorescence-labeled oligonucleotides in the case of FISH). It is also desirable to stretch the whole set of chromosomes from a cell without being mixed up with DNA from other cells. The authors have previously demonstrated the stretching of DNA fibers in a fluid-shear field created by electroosmotic flow (EOF) [2]. However, still remaining problems were, 1) cells are randomly placed, and DNA fibers drawn from these cells often overlap with each other, and 2) the stretched DNA fiber cannot be immobilized stably, and coils back to unstretched shape when EOF is turned off. In this paper, we propose and demonstrate the use of micro-structures for 1) positioning of cells at predetermined sites on a substrate, one at a site, and 2) maintaining stretched DNA fibers even after EOF is turned off.

2. Positioning of cells

For the positioning of individual cells onto a substrate, we use an array of triangular pillars having the minimum spacing of 2μm and made of 10μm height SU-8 photo polymer (Microchem. Corp.), as shown in Fig. 1.The array is located at the center of a micro-chamber (Fig. 1 a) equipped with a pair of electrodes to create EOF. The chamber is filled with a buffer, and cell suspension is fed from the entrance side (left in Fig. 1 a) of the array, and a voltage (20V across 5cm electrode spacing) is applied. The cell used in the experiment is the fission yeast, *S. pombe*, having an ellipsoidal shape of approximately 3μm x 3μm x 10μm. The cell, settling down to the bottom and carried by EOF, goes into the gap of the triangular pillar array, and because it is larger than the minimum spacing, it is trapped there (Fig. 2 a). The trapped cell blocks the flow through the gap, and the flow pattern changes, so that next incoming cells must either go over the pillar or go into the neighboring gap,

thus only one cell is trapped at a gap. Fig. 2 b) and c) are the photos of the trapped cells after flushing free cells, showing that cells are neatly positioned on the gaps, one at a place.

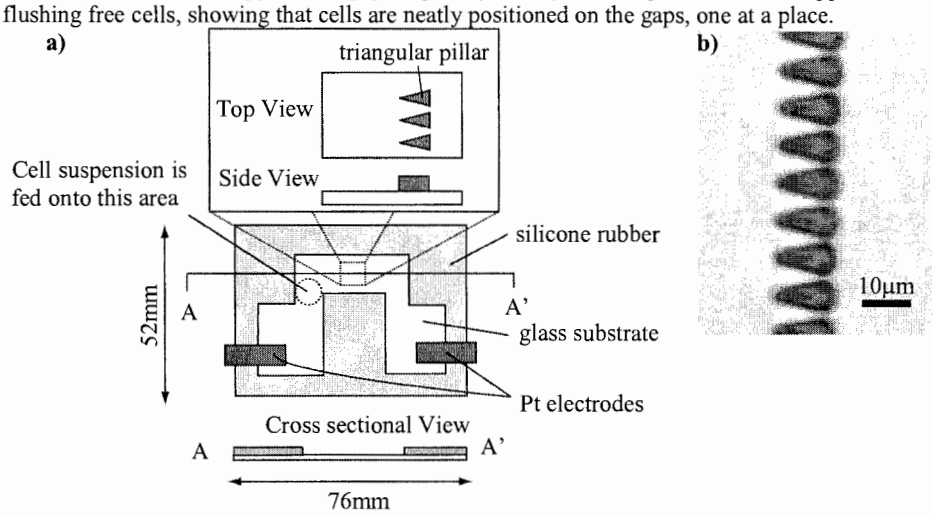

Fig. 1. a) Flow chamber for uni-directional EOF, having an array of triangular pillars fabricated on glass substrate. **b)** Microscopic image of the triangular pillars.

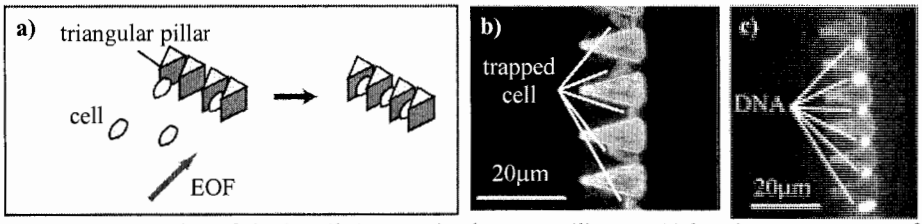

Fig. 2. a) Positioning of single cells by trapping between pillars. **b)** Light microscope image of trapped cell. **c)** Fluorescence image of DNA in the cell.

3. Maintaining stretched DNA fibers

The stretched DNA fiber coils back to random conformation when EOF is turned off. To maintain stretched shape even after the removal of EOF, we use micro-pillars, around which DNA fibers are wound, as schematically shown in Fig.3.

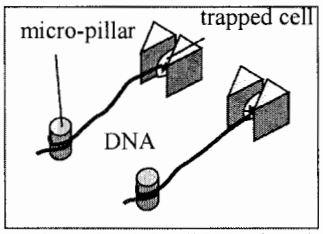

Fig. 3. Maintaining DNA fibers by winding it around pillars

Fig. 4 a) shows the device for this purpose, consisting of two pairs of electrodes (A-D) in a flow chamber. The procedure is as follows. 1) By applying voltage to the electrodes, A positive and C negative, EOF from A to C is created, and the cells are positioned at the triangular pillars. 2) With EOF C→A, DNA fiber is stretched out (Fig.4 b1). 3) With EOF D→B, the fiber is pushed against the sidewall of the pillar (Fig.4 b2), 4) the rotating EOF is created by sequentially switching the voltage in such a way that

A→C (Fig.4 b3), B→D (Fig.4 b4), C→A (Fig.4 b5), and the fiber is wound around the pillar to be immobilized.

Thus the fiber is suspended bridging over the triangular and the circular pillar, while the middle part of the fiber is held without contact to the solid surface, allowing free access of foreign molecules without steric hindrance. Such configuration is expected to realize high-resolution high-efficiency FISH.

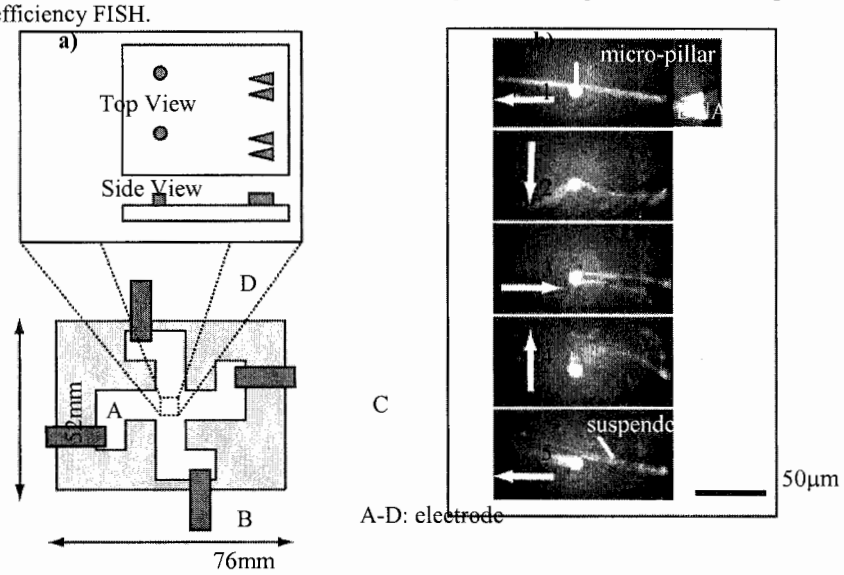

Fig. 4. a) Flow chamber for rotating EOF. Insert shows micro-pillars on the glass substrate. **b)** Winding of DNA fibers around a pillar with the rotating EOF (arrow)

5. Conclusions

With the use of EOF in combination with microfabricated structures, we have demonstrated 1) the positioning of cells at a predetermined site on a substrate, one at a site, 2) drawing DNA fibers out of each cell, and 3) winding of DNA fiber around pillars by rotating EOF. The stretched DNA fibers are suspended between the pillars to allow free access of foreign molecules in such a process as FISH.

Acknowledgements

The authors would like to thank Dr. Kimihilko Sugaya of the National Institute of Radiological Sciences for providing the fission yeast strain. This work is supported by BRAIN (Seiken Kiko) Research and Development Program for New Bio-industry Initiatives, and by Grant-in-Aid for Scientific Research on Priority Areas (C) "Genome Science" from the Ministry of Education, Culture, Sports, Science and Technology of Japan (no. 13202028, 14011225, and 15011200). Photography masks were fabricated using EB lithography apparatus of VLSI Design and Education Center (VDEC), The University of Tokyo.

References

[1] X. Michalet et al., *Science,* **277**, 1518-1523 (1997).

[2] M. Washizu, Y. Nikaido and H. Kabata, *Journal of Electrostatics*, **57**, 397-405 (2003).

UTILIZATION OF CELL-SIZED LIPID CONTAINERS FOR NANOSTRUCTURE AND SINGLE MOLECULE MANIPULATION

Guillaume Tresset[1] **and Shoji Takeuchi**[2]
[1]*LIMMS/CNRS-IIS,* [2]*CIRMM/IIS*
The University of Tokyo, 4-6-1 Komaba, Meguro-ku, Tokyo 153-8505, Japan
E-mail: takeuchi@iis.u-tokyo.ac.jp

Abstract

This paper proposes an original approach to handle submicrometer-sized biological or artificial materials for micro total analysis applications. After the enclosure of nanoparticles or DNA inside a cell-sized lipidic vesicle, it becomes possible to manipulate these objects as readily as cells within a microdevice equipped with electrode arrays, and to monitor the operations by conventional optical detection systems. Fusion of different liposomes by silicon micromachined electrodes has been demonstrated and opens up the route to ultra-small biomimetic reactors controlled in MEMS devices.

Keywords: liposome, DNA, nanoparticle, electroosmotic flow, electrofusion

1. Introduction

With the remarkable technical advances made in nanostructure fabrication and single molecule isolation [1], new strategies are to be elaborated to manipulate these objects in view of high throughput reactions and analyses performed in microfluidic devices. Due to their tiny dimensions and to the Brownian motion, observation and individual control of nanoobjects in suspension require sophisticated apparatus (e.g. optical tweezers) not always compatible with routine operations.

For several years, synthetic lipid-bilayer containers, the so-called liposomes, have been widely used in biotechnology as delivery vehicles of drug and gene [2]. Cell-sized liposomes can be easily prepared in large amount with any sort of material inside. This compartmentalization has dramatic advantages: i) vesicles protect materials inside from the environment, which is an important feature for constructing future artificial cells [3], ii) handling of nanoobjects becomes as straightforward as with cells, iii) fusion of two reactant-loaded liposomes should allow to trigger reactions more efficiently thanks to the small enclosing volume [4]. Liposome electrofusion has been already proven in previous experiments [5]: with silicon micromachined electrodes, various fluorescent liposomes were fused together at a success rate up to 75 % for DC pulses of electrical field typically around 10 $kV.cm^{-1}$.

The two new aspects of our work will be accordingly introduced, i.e. encapsulation of materials and manipulation of liposomes in microfluidic device.

2. Encapsulation of DNA and nanoparticles into liposomes

Liposomes were obtained after the 'reverse-phase evaporation' protocol [6] from a mixture of phospholipids (Sigma) and lipophilic fluorescent dye DiO or DiI (Molecular Probes), diluted in chloroform and methanol 2:1. A dry lipidic film was made by rotary evaporation under high vacuum. After moisturization by buffer (5 mM $MgCl_2$, 200 mM glucose, pH~7.5) containing λ-DNA (Takara) at 10^{11} molecules/mL and SYBR Green (Molecular Probes), 10 μm-average large liposomes were formed entrapping some of the surrounding fluorescent-stained molecules.

Figure 1 gives a fluorescent image of DNA-loaded liposomes taken just after that preparation. 40 % to 50 % of liposomes larger than 5 μm contained at least one λ-DNA molecule. In order to prove DNA was really enclosed and protected from the environment by the liposome membrane, we put 1 mg/mL of DNase I (Roche) – an enzyme which digests DNA and accordingly stops its

fluorescence – into the liposome solution. For comparison, we prepared another liposome solution, but this time DNA was injected after the formation of liposomes so that it cannot be enclosed inside them. Figure 2 shows the decay of fluorescence in both cases. After 5 hours, even though all DNA was not completely digested, the steady-state fluorescence intensity in the first case was larger than in the case where DNA was only outside the liposomes. This result indicates that after digestion a fraction of DNA is confined in liposomes and protected from the DNase. In the first case again, we checked thereafter the enzyme was still active by adding a small amount of DNA: as expected, fluorescence transiently increased then decayed due to the enzyme activity down to the same level as before.

The same process was also applied to trap 200 nm polystyrene spheres. Like λ-DNA, the nanoparticles could move freely while remaining confined by the liposome membrane (Figure 3). Therefore, biological materials but also inorganic structures can be contained by liposome with excellent sealing properties.

3. Liposome manipulation

Figure 4 exemplifies the concept of single molecule manipulation. A DNA molecule is encapsulated into a 'giant' liposome which serves as a conveyor traveling through a flow channel. The actuation is carried out by an array of microelectrodes generating standard or traveling-wave dielectrophoresis.

To convey the previously loaded liposomes, we have designed a PDMS microfluidic channel on a microarray of gold electrodes. Four layers of AZ4620 thick photoresist (Clariant), patterned directly on the chip, were used as a sacrificial layer for the molding of PDMS (Figure 5). It can be seen on Figure 6 that this process allows to align precisely a thick, narrow and long channel on micropatterns. As a proof of principle, standard electroosmotic flow was achieved by connecting electrodes A and A' at the ground and by applying a 5 V/3 MHz AC potential on electrode B' (Figure 7).

4. Conclusions

Biological or inorganic submicrometer materials have been successfully entrapped inside cell-sized lipid containers, which act as a barrier against the outside environment. The manipulation and observation of these nanoobjects have been made easier by the utilization of these micrometer-sized liposomes, which can be moved or even fused thanks to conventional electrical techniques. Encapsulation, manipulation and fusion will be soon integrated on a same chip for using liposomes as ultra-small reactors. Self-assembly of nanostructures or gene expression from DNA could then take place in a controlled manner through the electrofusion of reactant-loaded liposomes.

Acknowledgements

The authors would like to thank Prof. H. Noji, Dr. Y. Rondelez and Dr. T. Yamamoto for their technical support and fruitful discussions. Some of the micromachining processes have been accomplished with the support of Prof. H. Fujita. This work was partly supported by the Japan Society for the Promotion of Science (JSPS) and by the PROgram for the Promotion of Basic Research Activities for Innovative Biosciences (PROBRAIN) under the supervision of the Ministry of Agriculture and Fisheries in Japan.

References

[1] G.M. Whitesides, *Nature Biotechnology*, **21**, 1161-1165 (2003).
[2] A.S. Ulrich, *Bioscience Reports*, **22**, 129-149 (2002).
[3] J.W. Szostak, D.P. Bartel, and P. Luigi Luisi, *Nature*, **409**, 387-390 (2001).
[4] D.T. Chiu et al, *Science*, **283**, 1892-1895 (1999).
[5] G. Tresset and S. Takeuchi, to be published in *Biomedical Microdevices*.
[6] *Liposomes*, edited by V.P. Torchilin and V. Weissig, 2nd Edition, Oxford University Press, 2003.

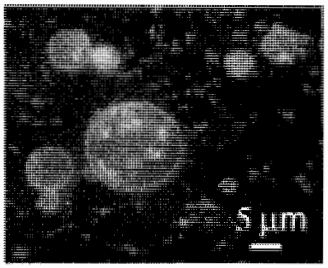

Figure 1. Fluorescent image of DNA-loaded liposomes. Green dots stand for λ-DNA molecules whilst lipids are labeled in red.

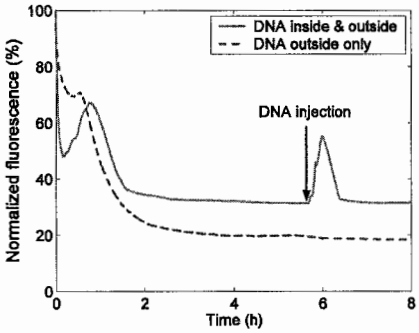

Figure 2. λ-DNA digestion by DNase I with DNA inside and outside liposomes, and DNA outside only. In the first case, small amount of DNA is injected to verify the viability of the enzyme. The fluorescence of SYBR Green is recorded at 520 nm under excitation at 497 nm.

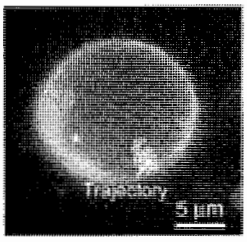

Figure 3. Trajectory of a 200 nm fluorescent red bead confined inside a fluorescent green liposome.

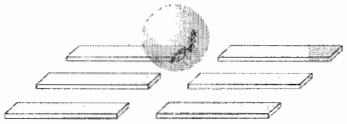

Figure 4. Concept of DNA manipulation: the molecule is enclosed inside a cell-sized liposome which is in turn handled by an array of microelectrodes inducing dielectrophoretic forces.

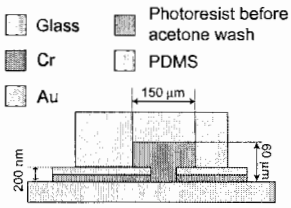

Figure 5. Schematic cross-section of the device with its components.

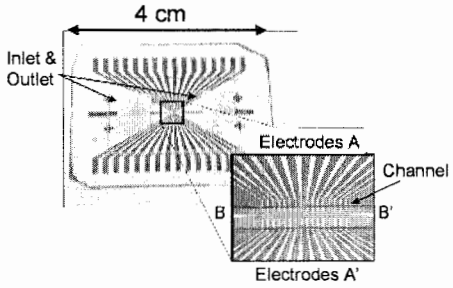

Figure 6. Photograph of the device and close-up view of the electrode array.

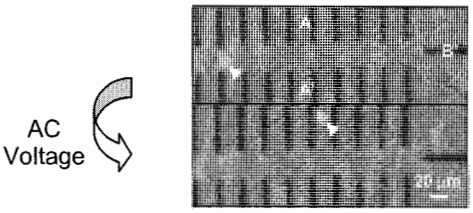

Figure 7. Electroosmotic flow on a red fluorescent liposome in a microfluidic device. The voltage is applied between B' and (A, A').

DEVELOPMENT OF INDIVIDUAL CELL SORTING SYSTEM FOR INTERCELLULAR REACTION ANALYSIS

Shin-ichiro Otsuka[*1], Masaki Kanai[1,2], Masahiro Hayashi[1], Hiroaki Nakanishi[2], and Shuichi Shoji[1]

*[*1]Major in nanoscience and nanoengineering, Waseda University, 3-4-1,Okubo,Shinjuku,Tokyo 169-8555,Japan*

[2]Technology Research Laboratory, Shimadzu Corporation, 3-9-4,Hikari-dai,Seika-cho,Soraku-gun,Kyoto 619-0237,Japan

Abstract

We developed a prototype of the cell sorting system for the intercellular reaction analysis, which can sort two kinds of cells individually. To realize the functional sorting, innovative concepts of the asymmetric sheath flow and the additional protection flow were proposed in the 2-D sheath flow system. In the evaluations of the fabricated system, two kinds of fluorescent beads were selectively introduced to the diagnostic chamber using on chip micro valves. In additional, a multiple sorting system having four outlet chambers was also fabricated. Basic sample injection behaviors were evaluated. These devices are applicable for not only the intercellular reaction analysis but also the high-throughput multiple cell analysis.

Key words: cell analysis, cytokine, cell sorter, sheath flow, on chip micro valve

1. Introduction

In recent years, a lot of chip devices for cell analysis have been reported. One of the target is to observe cell reaction which concerns to the human diseases. In our research, we focus on the chip devices for intercellular reaction, so-called cytokine reaction which plays important roles on allergy, rheumatism, and many human diseases. In order to analyze these intercellular reactions, a cellular analysis system which can handle various cells individually is quite helpful. The methods which can handle the individual cell, such as laser tweezers and on-chip cell sorters using sheath flow have been reported so far. The laser tweezer can handle individual cell easily, however, its throughput is poor in practical use. While, the sheath flow cell sorter can achieve high-throughput operation and is easy to extend to a multiple handling system due to its simple structure. Conventional cell sorters mainly target the high throughput cell handling or the single-species handling with good accuracy. In this paper, we developed the cell sorting system which can handle two different cells one by one. Prototype of the multi-outlet cell sorting system was also described.

2. Theory

Fig 1 shows the mechanism of the first prot
of cells are introduced to the sorting zone ir
Fig .1a and mode3; Fig .1b) and introduced t
The sheath buffer flows are switched using
cell sorter chip. In previous works, we alre
time was about 150msec [1,2].

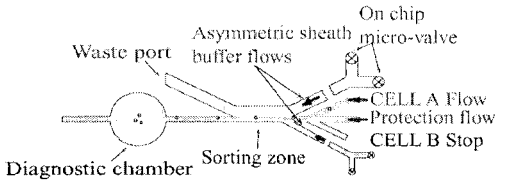

(a)Mode1: CELL A to chamber

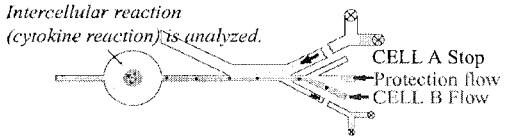

(b) Mode3: CELL B to chamber

Figure 1. Mechanism of the prototype cell sorter

This device has two innovative concepts of the 2-D sheath flow system that are the asymmetric sheath flow and the additional protection flow. An asymmetric channel structure of the sheath buffer flows improves the directional controllability of the cell flow. The cell flow is controlled by not only the sheath buffer flow but also the protection flow (center flow). The protection flow realizes a virtual wall to prevent the cell from flowing into the other cell inlet as shown in Fig 1.

3. Experimental

The prototype device having one diagnostic chamber and two-cell inlets were designed and fabricated based on the CFD (computational fluid dynamics) simulation results. A silicon was etched to form channels and through holes using deep RIE and anodically bonded with a Pyrex glass (#7740). A diaphragm of silicone rubber was bonded to the Si structure to fabricate pneumatic on chip micro valve [2].

As a pilot study, we evaluated switching behaviors of the fluorescent dyed water (10μM RhodamineB). A dyed water was injected to the device using syringe pump, and was switched by the on chip micro valves. Next, we demonstrated the sorting of 6μm green and red fluorescent beads.

4. Result and discussion

Switching behaviors of the prototype cell sorter is shown in Fig .2. Fig .2a is switching from mode1 (cell A injection) to mode2 (cell A waste), while Fig .2b is from mode3 (cell B injection) to mode4 (cell B waste). The flows switched successfully with in 150msec using on chip micro valve. The protection flow avoids reverse flow to the other cell inlet effectively. Fig .3 shows the time dependant results of individually sorted beads to the same diagnostic chamber. Individual two kinds of beads sorting was confirmed. We achieved controlling the number of the beads sorted to the diagnostic chamber. The result shows the feasibility of the controllable cell collection with various combinations.

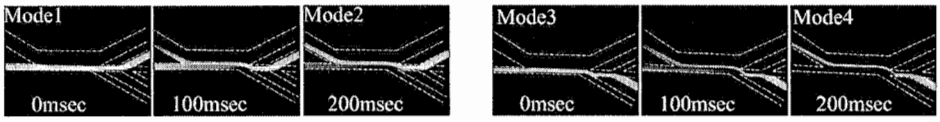

(a) Switching from mode1 to mode2 (b) Switching from mode3 to mode4

Figure 2. Switching evaluation using on chip valve

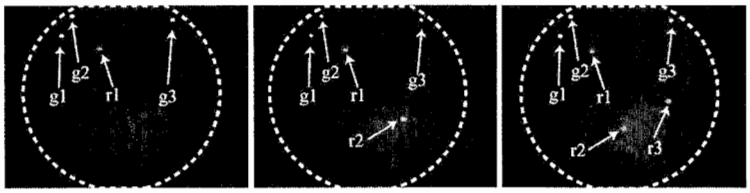

(a) 3 green beads 1 red bead (b) 3 green beads 2 red beads (c) 3 green beads 3 red beads

Figure 3. Beads injection to the diagnostic chamber. Individual red beads (CELL B) injections after injection of three green beads (CELL A).

We extended the concept of the prototype cell sorter chip to multiple cell sorter. Fig .4 shows the

other prototype cell sorter chip having multiple outlet chambers (four diagnostic chambers and two cell inlets) for the high-throughput multiple cell analysis. Four switching modes to the diagnostic chambers were realized successfully (Fig .4b). The concept of this system can be applicable for intercellular reaction analysis which requests introduction of the reagent to the cell collection chambers. The improvements of controllability of the multi cell sorter are under investigation.

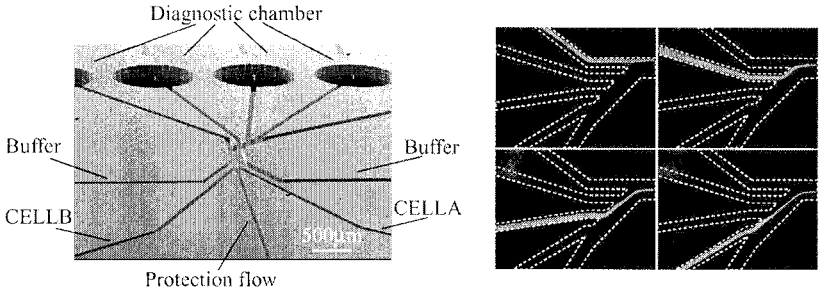

(a) SEM image of prototype device (b) Evaluated switching behavior

Figure 4. Prototype cell sorter chip of multiple chambers

5. Conclusions

We have developed a cell sorting system, which can sort two kinds of cells individually. The concepts of an asymmetric sheath buffer flow and an additional protection flow were proposed for the functional sorting. In the prototype device, selective sorting of two kinds of beads were realized successfully. We fabricated the multiple cell sorter and demonstrated a switching behavior. The 2D-sheath flow concepts proposed in this paper can be applicable for intercellular reaction analysis as well as the high-throughput multiple cell analysis.

Acknowledgements

This work is partly supported by Japan Ministry of Education, Culture, Sport Science & Technology Grant-in-Aid for COE Research and 21st COE of Waseda University, Scientific Basic Research (A) No. 12450167.and Japan Society for the Promotion Science Grant-in-Aid for Creative Scientific research No. 13GS0024.

References

[1] M.Kanai, S,Ikeda, J.Tanaka, J.S.Go, H.Nakanishi, S.Shoji *Sensors & Actuators A* 111 (2004) pp32-36

[2] M.Kanai, S,Otsuka, H,Nakanishi, S,Shoji, *Japanese Journal of Applied Physics,* Vol. 43, No. 6B, *in press*

CAPILLARY-ASSEMBLED MICROCHIP (CAs-CHIP) : A NEW METHOD FOR INTEGRATING MULTIPLE CHEMICAL FUNCTIONS ONTO A SINGLE MICROFLUIDIC DEVICE

Hideaki Hisamoto [1], Yuya Nakashima [1], Chihiro Kitamura[1], Shun-ichi Funano [1], Midori Yasuoka [1], Keisuke Morishima [2], Yoshikuni Kikutani [2], Takehiko Kitamori [2,3], and Shigeru Terabe [1]

[1] Graduate School of Material Science, University of Hyogo, 3-2-1 Kouto, Kamigori-cho, Ako-gun, Hyogo 678-1297, Japan

[2] Micro Chemical Group, Kanagawa Academy of Science and Technology, 3-2-1 Sakado, Takatsu-ku, Kawasaki, Kanagawa 213-0012, Japan

[3] Department of Applied Chemistry, Graduate School of Engineering, The University of Tokyo, 7-3-1 Hongo, Bunkyo-ku, Tokyo 113-8656, Japan

Abstract

A novel concept of assembling various chemical functions onto a single microfluidic device is proposed. The concept, "CAPILLARY-ASSEMBLED MICROCHIP (CAs-CHIP), involves embedding chemically functionalized square capillaries onto a lattice microchannel network fabricated on polydimethyl siloxane (PDMS) possessing same channel dimensions to outer dimensions of square capillaries (Figure 1). This approach would allow easy fabrication of chemically-functionalized microfluidic device by freely embedding functional square capillaries on PDMS microchannel network. Here we report a fabrication method of CAs-CHIP, and an application for preparing a multiple chemical sensing chip as an example.

Keywords: chemical function, PDMS microchip, sensor, square capillary, surface modification

1. Introduction

Recently, integration of chemical functions onto microfluidic device has become a target of much current research in analytical chemistry. Many kinds of position-selective immobilization techniques such as a laminar flow patterning, photo polymerization were reported by many groups [1-3].

These techniques are quite promising for integrating a single chemical function onto a microfluidic device; however, an experimental difficulty arises when different and plural chemical functions are integrated into a single microfluidic device. This is because most techniques listed above require introduction of reagent solutions into the "whole microchannel", although the chemical modification is only carried out at a defined position of it. Therefore, in general, once a certain chemical function is patterned at part of the channel, position-selectively, other reagents should be introduced over another patterned surface to integrate plural chemical functions into a single microchannel. This may lead to contamination or deterioration of the previously patterned chemical function. Here we propose a simple and promising approach for assembling various chemical functions onto a single microfluidic device as shown in Figure 1. Our concept, called a capillary-assembled microchip (CAs-CHIP), involves embedding of chemically functionalized square capillaries into the lattice microchannel network fabricated on PDMS having the same channel dimensions as the outer dimensions of the square capillaries[4]. Here we report the first example implementing the concept and we give a simple example application of the method for preparing a dual chemical sensing chip which can measure pH and calcium ion simultaneously.

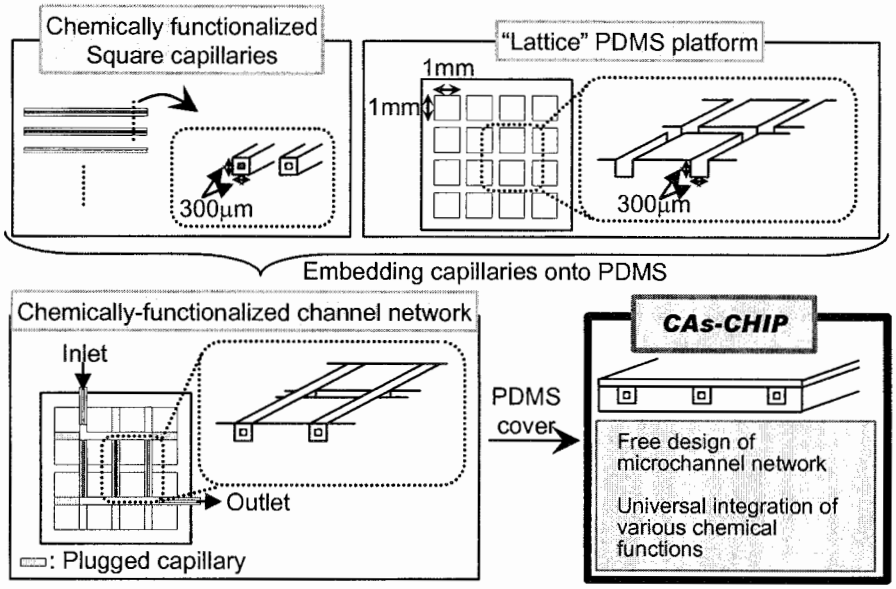

Figure1 General concept for preparing CAs-CHIP

2. Experimental

Square capillaries were cut into appropriate lengths (usually one to three millimeters) and embedded into the lattice microchannel network fabricated on the PDMS plate. Plugged capillaries were prepared by introduction of PDMS prepolymer into square capillaries (inner width: 50 μm) and cured at 70 °C for more than 5 h. These plugged capillaries were also cut and used for preparing the designed channel network. After embedding all the capillaries, a PDMS cover was bonded on top. For this, a spin-coated PDMS prepolymer on a glass slide was used as a cover plate. PDMS prepolymer was spin coated on the glass slide at 5000 rpm, then adhered to the capillary-embedded PDMS plate with clippers before curing. Bonding was carried out by curing at 70 °C for 5 h. The chemical sensing capillaries for pH and calcium ion were prepared by immobilizing respective sensing membranes to inner surface of capillaries.

3. Results and discussion

Figure 2 shows the preliminary design of the microchip for dual chemical sensing. By using spin-coated PDMS prepolymer as a cover plate, fabrication of a capillary-embedded microchannel (capillary) network without any solution leakage was successfully performed. For sensing application, we have prepared pH and calcium ion-sensing capillaries by attaching hydrogel-based membrane and plasticized PVC membrane to inner surface of square capillaries, and embedded them into PDMS chip. When the sample solution passed through the sensing capillaries, the fluorescence of each membrane changed by selective interaction with each analyte. The most characteristic feature of this chip is that the different type of capillaries can be embedded onto a single microfluidic device.

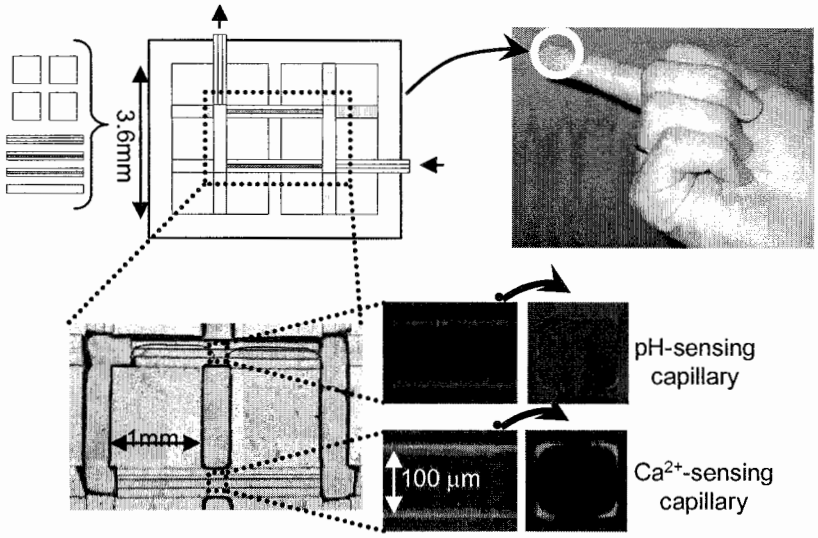

Figure2 Preparation of dual-sensing CAs-CHIP

4. Conclusions

We have proposed a novel concept for assembling various chemical functions onto a single microfluidic device, called a capillary-assembled microchip (CAs-CHIP). By employing spin-coated PDMS prepolymer, we fabricated a capillary-embedded microchannel (capillary) network with no solution leakage. Two different types of chemical sensing layers were prepared inside the square capillaries, and these modified capillaries were embedded into a lattice PDMS channel network to fabricate a parallel dual-sensing microchip. Many types of surface modification methods inside capillaries are well known, so that the proposed method has great potential to fabricate different microfluidic devices having various chemical functions for analytical or synthetic applications.

Acknowledgements

This work was partially supported by Grants for Scientific Research from the Ministry of Education, Culture, Sports, Science and Technology, Japan, Kawanishi Memorial Shinmeiwa Education Foundation, Japan.

References

[1] P.J.A. Kenis, R.F. Ismagilov, G.M. Whitesides, *Science.*, **285**, 83-85, (1999).
[2] J. Moorthy, D.J. Beebe, *Anal. Chem.*, **75**, 292A-301A, (2003).
[3] H. Hisamoto, Y. Shimizu, K. Uchiyama, M. Tokeshi, Y. Kikutani, A. Hibara, and T. Kitamori, *Anal. Chem.*, **75**, 350-354, (2003).
[4] H. Hisamoto, Y. Nakashima, C. Kitamura, S.-i. Funano, M. Yasuoka, K. Morishima, Y. Kikutani, T. Kitamori and S. Terabe, *Anal. Chem.*, **76**, 3222-3228, (2004).